
ProteinGym: Large-Scale Benchmarks for Protein Design and Fitness Prediction

Pascal Notin^{†*}
Computer Science,
University of Oxford

Lood van Niekerk[†]
Systems Biology,
Harvard Medical School

Nathan Rollins
Seismic Therapeutic

Jonathan Frazer
Centre for Genomic Regulation
Universitat Pompeu Fabra

Rose Orenbuch
Systems Biology,
Harvard Medical School

Aaron W. Kollasch[†]
Systems Biology,
Harvard Medical School

Steffanie Paul
Systems Biology,
Harvard Medical School

Ada Shaw
Applied Mathematics,
Harvard University

Mafalda Dias
Centre for Genomic Regulation
Universitat Pompeu Fabra

Yarin Gal
Computer Science,
University of Oxford

Daniel Ritter[†]
Systems Biology,
Harvard Medical School

Hansen Spinner
Systems Biology,
Harvard Medical School

Ruben Weitzman
Computer Science,
University of Oxford

Dinko Franceschi
Systems Biology,
Harvard Medical School

Debora S. Marks^{*}
Harvard Medical School
Broad Institute

Abstract

Predicting the effects of mutations in proteins is critical to many applications, from understanding genetic disease to designing novel proteins that can address our most pressing challenges in climate, agriculture and healthcare. Despite a surge in machine learning-based protein models to tackle these questions, an assessment of their respective benefits is challenging due to the use of distinct, often contrived, experimental datasets, and the variable performance of models across different protein families. Addressing these challenges requires scale. To that end we introduce ProteinGym, a large-scale and holistic set of benchmarks specifically designed for protein fitness prediction and design. It encompasses both a broad collection of over 250 standardized deep mutational scanning assays, spanning millions of mutated sequences, as well as curated clinical datasets providing high-quality expert annotations about mutation effects. We devise a robust evaluation framework that combines metrics for both fitness prediction and design, factors in known limitations of the underlying experimental methods, and covers both zero-shot and supervised settings. We report the performance of a diverse set of over 70 high-performing models from various subfields (eg., alignment-based, inverse folding) into a unified benchmark suite. We open source the corresponding codebase, datasets, MSAs, structures, model predictions and develop a user-friendly website that facilitates data access and analysis.

*Correspondence: pascal.notin@cs.ox.ac.uk, kollasch@g.harvard.edu, danielritter1@gmail.com, loodvn@gmail.com, debbie@hms.harvard.edu ; † Equal contribution

1 Introduction

Proteins carry out a wide range of functions in nature, facilitating chemical reactions, transporting molecules, signaling between cells, and providing structural support to cells and organisms. This astonishing functional diversity is uniquely encoded in their amino acid sequence. For instance, the number of possible arrangements for a 64-residue peptide chain (20^{64}) is already larger than the estimated number of atoms in the universe. Despite substantial progress in sequencing over the past two decades, we have observed a relatively small, biased portion of that massive sequence space. Consequently, the ability to manipulate and optimize known sequences and structures represents tremendous opportunities to address pressing issues in climate, agriculture and healthcare.

The design of novel, functionally optimized proteins presents several challenges. It begins with learning a mapping between protein sequences or structures and their resulting properties. This mapping is often conceptualized as a “fitness landscape”, a multivariate function that characterizes the relationship between genetic variants and their adaptive fitness. The more accurately and comprehensively we can define these landscapes, the better our chances of predicting the effects of mutations and designing proteins with desirable and diverse properties. Machine learning, by modeling complex, high-dimensional relationships, has emerged as a powerful tool for learning these fitness landscapes. In recent years, a plethora of machine learning methods have been proposed for protein modeling, each promising to offer new insights into protein function and design. However, assessing the effectiveness of these methods has proven challenging. A key issue is their evaluation on distinct and relatively sparse benchmark datasets, while relative model performance fluctuates importantly across experimental assays, as was shown in several prior analyses [Riesselman et al., 2018, Laine et al., 2019, Meier et al., 2021]. This situation underscores the importance of scale in the benchmarks used. Larger, more diverse datasets would offer a more robust and comprehensive evaluation of model performance.

To address these limitations, we introduce ProteinGym, a large-scale set of benchmarks specifically tailored to protein design and fitness prediction. It comprises a broad collection of over 250 standardized Deep Mutational Scanning (DMS) assays which include over 2.7 million mutated sequences across more than 200 protein families, spanning different functions, taxa and depth of homologous sequences. It also encompasses clinical benchmarks providing high-quality annotations from domain experts about the effects of $\sim 65k$ substitution and indel mutations in human genes (§ 3).

We have designed ProteinGym to be an effective, holistic, robust, and user-friendly tool. It provides a structured evaluation framework that factors in known limitations of the underlying experimental methods and includes metrics that are tailored to protein design and mutation effect prediction (§ 4). We report the performance in a unified benchmark of over 70 diverse high-performing models that come from various subfields of computational biology (e.g., mutation effects prediction, sequence-based models for de novo design, inverse folding), thereby supporting novel comparisons across. Unlike prior benchmarks, ProteinGym integrates both the zero-shot and supervised settings, leading to new insights (§ 5). All models are codified with a common interface in the same open-source codebase, promoting consistency and ease of use. Lastly, a dedicated website offers an interactive platform to facilitate comparisons across datasets and performance settings.

2 Related Work and Background

Multi-task protein benchmarks In recent years, several benchmarks have been introduced to provide initial means to assess protein model performance across a multitude of tasks of interests, e.g., predicting contacts, structure, thermostability, and fitness. These benchmarks are generally geared towards assessing the quality of learned protein representations, and the extent to which these representations can be broadly leveraged for various tasks. However, for fitness prediction, they all rely on a very limited set of proteins (e.g., 1-3 assays). In comparison, the ProteinGym benchmarks focus on a single task – fitness prediction – and encompass *two orders of magnitude more* point mutations assessed and vast diversity of protein families included.

TAPE (Tasks Assessing Protein Embeddings) [Rao et al., 2019] covers five protein prediction tasks, each designed to test a different aspect of protein function and structure prediction (secondary structure, contact, remote homology, fluorescence and stability), and focuses on assessments in the semi-supervised regime via carefully curated train-validation-test splits. ProteinGLUE [Capel et al.,

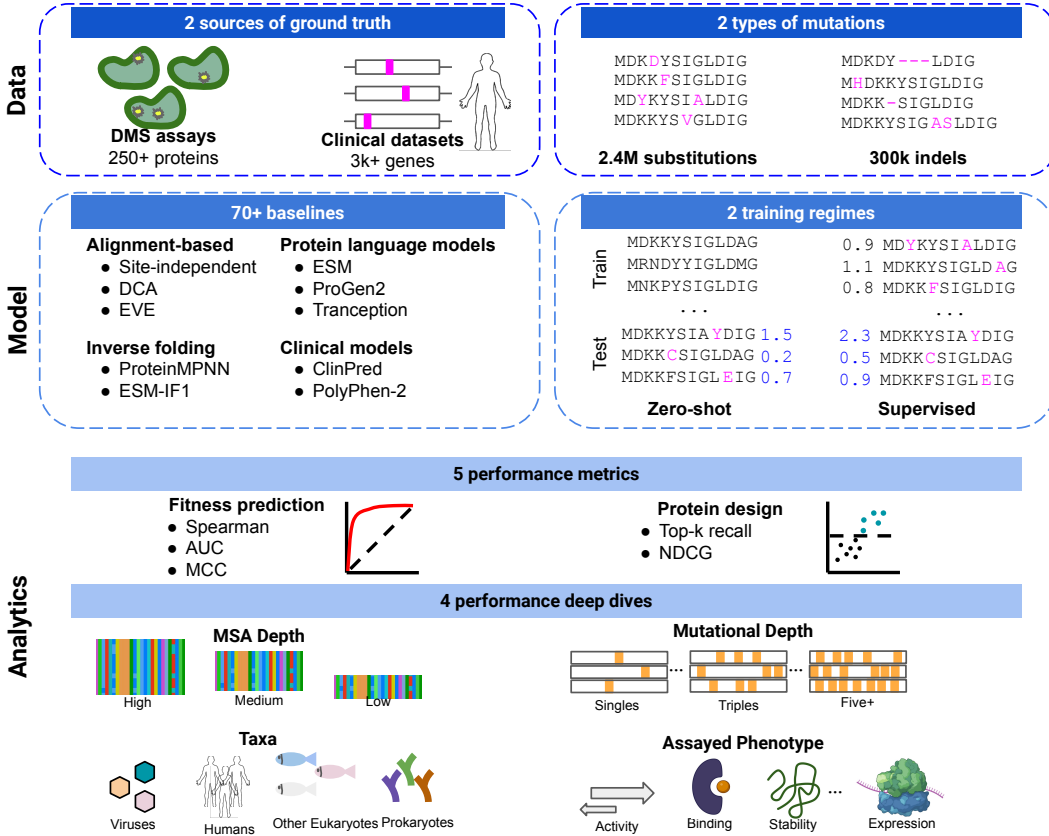


Figure 1: ProteinGym benchmarks ProteinGym is comprised of three layers. The data layer encompasses two complementary ground truth labels from DMS assays and clinical annotations from experts. For both, we analyze two types of mutations: substitutions and indels. The model layer is comprised of a diverse set of baselines, tailored to both zero-shot and supervised training regimes. Lastly, the analytics layer includes several performance metrics geared towards fitness prediction or protein design evaluation. Different segmentation variables (e.g., MSA depth, assayed phenotype, taxa) facilitate the comparisons of models across diverse settings

2022] also focuses on assessing the usefulness of learned protein representations on supervised downstream tasks. It is comprised of five different tasks, none directly related to protein fitness: secondary structure, solvent accessibility, protein-protein interactions, epitope region and hydrophobic patch prediction. PEER [Xu et al., 2022] also focuses on multi-task benchmarking, grouped in five categories: protein property, localization, structure, protein-protein interactions and protein-ligand interactions. It contains a richer set of evaluations compared with the prior two benchmarks, and also investigates the multi-task learning setting, but is not designed for thorough fitness prediction benchmarking (3 fitness related assays). The handful of fitness DMS assays from these various benchmarks are all subsumed in ProteinGym.

Single task, non-fitness datasets & benchmarks Efforts to create fair, large-scale, and comprehensive benchmarks have been a significant focus of computational biologists for certain tasks. Among these, the biennial Critical Assessment of protein Structure Prediction (CASP) [Kryshtafovych et al., 2021] is the most renowned. CASP concentrates on protein structure prediction and has set the gold standard in this domain. In parallel to CASP, the Critical Assessment of Functional Annotation (CAFA) [Zhou et al., 2019] challenge provides a platform for evaluating protein function classification. The SKEMPI [Moal and Fernández-Recio, 2012] database is specifically designed to aid the evaluation of computational methods predicting the effect of mutations on protein-protein binding affinity. Several datasets have been curated for specific properties of interest across a diverse set of

proteins, for instance thermostability [Tsuboyama et al., 2022, Stourac et al., 2020, Chen et al., 2022] or solubility [Hon et al., 2020].

Protein fitness benchmarks Closest to our work are the collections of DMS assays that were curated in Hopf et al. [2017] (28 substitution assays), and then further expanded upon in Riesselman et al. [2018] (42 substitution assays) and Shin et al. [2021] (4 indel assays). We include all assays related to fitness prediction from these prior works in ProteinGym. FLIP [Dallago et al., 2021] focused on comparing fitness predictors in the semi-supervised setting, developing a robust evaluation framework and curating cross-validation schemes for three assays. MaveDB [Rubin et al., 2021] is a repository rather than a benchmark, but it compiles a large collection of datasets from multiple variant effect mapping experiments that can be used for benchmarking purposes. An initial prototype of the ProteinGym benchmarks (referred to as ‘ProteinGym v0.1’) was introduced in Notin et al. [2022a]. We have since then significantly expanded the benchmarks in terms of number and diversity of underlying datasets, baselines, evaluation framework and model training regimes (Table A1). This not only enables performance evaluation at an unprecedented scale, but also builds connections between different subfields that are often perceived as separate, as we discuss in the following paragraph.

Clinical Benchmarks Designing an unbiased, non-circular and broadly applicable benchmark to evaluate the performance of human variant effect predictors at predicting clinical significance is still an open-problem for the clinical community. Combining DMS with clinical annotations has been a fruitful direction to avoid biases [Frazer et al., 2021, Livesey and Marsh, 2023]. ClinGen curated a clinical dataset specifically designed to compare a subset of models [Pejaver et al., 2022].

Relationship between protein fitness, mutation effect prediction and design The protein fitness landscape refers to the mapping between genotype (e.g., the amino acid sequence) and phenotype (e.g., protein function). While it is a fairly broad concept, it should always be thought about in practice within a particular context (e.g., stability at a given temperature in a specific organism). Models that learn the protein fitness landscape have been shown to be effective at predicting the effects of mutations [Frazer et al., 2021, Jagota et al., 2022, Brandes et al., 2023, Notin et al., 2022b]. But the ability to tell apart the sequences that are functional or not is also critical to protein engineering efforts [Romero et al., 2012, Yang et al., 2018, Wu et al., 2019, Alley et al., 2019b]. Although typically introduced in the context of de novo protein design [Huang et al., 2016], inverse folding methods [Ingraham et al., 2019, Jing et al., 2020, Dauparas et al., 2022, Gao et al., 2022] can also be used for mutation effects prediction (Appendix A.4.1). There is thus a very tight connection between protein fitness, mutation effect prediction and protein engineering, and the same models can be used for either task depending on context. We seek to illustrate this connection through this work, comparing baselines introduced in different fields (e.g., protein representation learning, inverse folding models, co-evolution models) on the same benchmarks, and including different metrics that are geared more to mutation effect prediction (e.g., Spearman) or design tasks (e.g., NDCG).

3 ProteinGym benchmarks

ProteinGym is a collection of benchmarks (Fig. 1) that cover different types of mutation (ie., substitutions vs. indels), ground-truth labels (ie., experimental measurement from DMS vs. clinical annotations), and model training regime (ie., zero-shot vs. supervised).

3.1 Mutation types

We curate benchmarks for two types of protein mutations – *substitutions* and *indels* (insertions or deletions), each with unique implications for the structure, function, and modeling of proteins.

Substitutions Substitution mutations refer to a change in which one amino acid in a protein sequence is replaced by another. Depending on the properties of the substituted amino acid, this can have varied impacts on the protein’s structure and function, which can range from minimal to drastic. The influence of a substitution largely depends on whether it is conservative (i.e., the new amino acid shares similar properties to the original) or non-conservative. In terms of computational modeling, substitutions are the most commonly addressed mutation type, and the majority of mutation effect predictors support substitutions.

Indels Indel mutations correspond to insertions or deletions of amino acids in protein sequences. While indels can affect protein fitness in similar ways to substitutions, they can also have profound impacts on protein structure by altering the protein backbone, causing structural modifications inaccessible through substitutions alone [Shortle and Sondek, 1995, Tóth-Petróczy and Tawfik, 2013]. From a computational perspective, indels present a unique challenge because they alter the length of the protein sequence, requiring additional considerations in model design and making it more difficult to align sequences. For instance, the majority of models trained on Multiple Sequence Alignments are typically unable to score indels due to the fixed coordinate system they operate within (see § 4). Furthermore, when dealing with probabilistic models, comparing relative likelihoods of sequences with different lengths results in additional complexities and considerations.

3.2 Dataset types

The fitness of a protein is a measure of how well a protein can perform its function within an organism. Factors that influence protein fitness are diverse and include stability, folding efficiency, catalytic activity (for enzymes), binding specificity and affinity. To properly capture this diversity, we curated a broad set of experimental assays that map a given sequence to phenotypic measurements that are known or hypothesized to be related to its fitness. We focused on two potential sources of ground truth: Deep Mutational Scanning (DMS) assays and Clinical datasets.

Deep Mutational Scanning assays Modeling protein fitness landscapes presents a challenge due to the complex relationship between experimentally measured protein fitness, the distribution of natural sequences, and the underlying fitness landscape. It is challenging to isolate a singular, measurable molecular property that reflects the key aspects of fitness for a given protein. In developing ProteinGym, we prioritized assays where the experimentally measured property for each mutant protein is likely to represent the role of the protein in organismal fitness. The resulting compilation of over 250 DMS assays extends over a wide array of functional properties, including ligand binding, aggregation, thermostability, viral replication, and drug resistance. It encompasses diverse protein families, such as kinases, ion channel proteins, G-protein coupled receptors, polymerases, transcription factors, and tumor suppressors. In contrast to most DMS assay collections that focus exclusively on single amino acid substitutions, ProteinGym includes several assays with multiple amino acid variants. Moreover, it spans different taxa (i.e., humans, other eukaryotes, prokaryotes, and viruses), alignment depths, and mutation types (substitutions vs indels). All details about the curation and pre-processing of these DMS assays are provided in Appendix A.3.

Clinical datasets ClinVar [Landrum and Kattman, 2018] is an extensive, public database developed by the National Center for Biotechnology Information (NCBI). It serves as an archival repository that collects and annotates reports detailing the relationships among human genetic variations and associated phenotypes with relevant supporting evidence, thereby providing robust, clinically annotated datasets that are invaluable for understanding the functional impact of mutations. From the standpoint of benchmarking mutation effects predictors, ClinVar permits the direct comparison of predictive models in terms of their accuracy in estimating the functional impact of mutations on human health. Annotations are also available for an order of magnitude more distinct proteins compared with our DMS-based benchmarks, albeit much sparser per protein (see table 1). In the case of indels, we focused on short (≤ 3 amino acids) variants. In ClinVar, 84% of indel annotations are pathogenic, so we added to our clinical dataset common indels from gnomAD (allele frequency $>5\%$) as pseudocontrols [Karczewski et al., 2020].

3.3 Model training regime

Lastly, we discriminate in our benchmarks between zero-shot and supervised settings. In the supervised regime we are allowed to leverage a subset of labels to train a predictive model, while in the zero-shot setting we seek to predict the effects of mutations on fitness without relying on the ground-truth labels for the protein of interest. These two settings offer complementary viewpoints of practical importance. For instance, in settings where labels are subject to several biases or scarcely available (e.g., labels for rare genetic pathologies), we need methods with robust zero-shot performance performance. In cases where we seek to design new proteins that simultaneously optimize several properties of interest (e.g., binding affinity, thermostability) and we have collected a sufficiently large number of labels for each target, supervised methods are more appropriate. The

Dataset	Description	Mutation type	# Proteins	# Mutants
DMS	High-throughput assays evaluating the functional impact of a wide range of protein mutations	Substitutions	217	2.4M
		Indels	66	0.3M
Clinical	Expert-curated clinical annotations across a wide range of human genes	Substitutions	2,525	63k
		Indels	1,555	3k
Total			3,422	2.7M

Table 1: **ProteinGym datasets summary** ProteinGym includes a large collection of DMS assays and clinical datasets that offer complementary viewpoints when assessing protein fitness. The table reports the number of mutants and unique proteins per dataset (the total being deduped across datasets).

need to rely on labels is even more pronounced when we seek to optimize several anti-correlated properties or when evolution is a poor proxy for the property of interest. Predictions obtained in the zero-shot settings may also be used to augment supervised models [Hsu et al., 2022a]. The two settings require substantially different evaluation frameworks, which we detail in § 4.

4 Evaluation framework

4.1 Zero-shot benchmarks

DMS assays In the zero-shot setting we predict experimental phenotypical measurements from a given assay, without having access to the labels at training time. Due to the often non-linear relationship between protein function and organism fitness [Boucher et al., 2016], the Spearman’s rank correlation coefficient is the most generally appropriate metric for model performance on experimental measurements. We use this metric similarly to previous studies [Hopf et al., 2017, Riesselman et al., 2018, Meier et al., 2021]. However, in situations where DMS measurements exhibit a bimodal profile, rank correlations may not be the optimal choice. Consequently, for these instances, we supplement our performance assessment with additional metrics, namely the Area Under the ROC Curve (AUC), and the Matthews Correlation Coefficient (MCC), which compare model scores with binarized experimental measurements. Furthermore, for certain goals (e.g., optimizing functional properties of designed proteins), it is more important that a model is able to correctly identify the most functional proteins, rather than capture the distribution of the full data. Thus, we also calculate the Normalized Discounted Cumulative Gains (NDCG), which up-weights a model if it gives its highest scores to sequences with the highest DMS value. We also calculate Top K Recall, where we select K to be the top 10% of DMS values. To avoid placing too much weight on properties where we have many assays (e.g. thermostability), we first compute each of these metrics within groups of assays that measure similar functions. The final value of the metric is then the average of these averages, giving each functional group equal weight.

Clinical datasets For the clinical data, with pathogenic and benign categories, we calculate the areas under the ROC and precision-recall curves. In the substitution dataset, 50% of the labels are in approximately 10% of the proteins. Since clinical labels across genes correspond to underlying pathologies that are very distinct to one another, it is preferable to assess performance on a gene-by-gene basis. We thus compute the average per-gene performance on the substitution benchmark. However, in the case of indels, only about half of the proteins has a pathogenic label (and only 10% have a both pathogenic and benign or pseudocontrol labels), so we compute the total AUC for the full dataset. The problem of calibrating model scores in a principled way across different genes is an open problem; we leave this to future work.

Baselines We implement a diverse set of 50+ zero-shot baselines that may be grouped into alignment-based models, protein language models, inverse folding models and ‘hybrid’ models. Alignment-based models, such as site-independent and EVmutation models [Hopf et al., 2017], DeepSequence [Riesselman et al., 2018], WaveNet [Shin et al., 2021], EVE [Frazer et al., 2021] and GEMME [Laine et al., 2019], are trained on Multiple Sequence Alignments (MSAs). Protein language models are trained on large quantities of unaligned sequences across protein families. They include UniRep [Alley et al., 2019a], the RITA suite [Hesslow et al., 2022], the ESM1 and ESM2

suite [Rives et al., 2021, Meier et al., 2021, Lin et al., 2023], VESPA [Marquet et al., 2022], the CARP suite [Yang et al., 2023a] and the ProGen2 suite [Nijkamp et al., 2022]. Inverse Folding models learn sequence distributions conditional on an input structure [Ingraham et al., 2019]. We include here ProteinMPNN [Dauparas et al., 2022] which is trained on structures in the PDB, MIF [Yang et al., 2023b] trained on CATH4.2 [Dawson et al., 2016], and ESM-IF1 [Hsu et al., 2022b] which is trained on the PDB and a dataset of AlphaFold2 folded structures. Hybrid models combine the respective strengths of family-specific alignment-based and family-agnostic language models, such as the MSA Transformer [Rao et al., 2021], evotuned UniRep [Alley et al., 2019a], Tranception [Notin et al., 2022a] and TranceptEVE [Notin et al., 2022b].

Because of the variable length of sequences subject to insertion or deletion mutations, alignment-based methods with fixed matrix representations of sequences are unable to score indels. However, profile Hidden Markov Model (HMM) and autoregressive models include explicit or implicit probabilities of indels at each position. Both are trained on homologous sequences recovered with an MSA and expanded to include insertions. The masked-marginals heuristic Meier et al. [2021] used to predict protein fitness with protein language models trained with a masked-language modeling objective (e.g., ESM-1v, MSA Transformer) does not support indels (see Appendix A.4). We thus only report the performance of the following baselines: Tranception [Notin et al., 2022a], TranceptEVE [Notin et al., 2022b], WaveNet [Shin et al., 2021], HMM [Eddy, 2011], ProGen2 [Madani et al., 2020], UniRep [Alley et al., 2019a], RITA [Hesslow et al., 2022] and ProtGPT2 [Ferruz et al., 2022].

For comparisons on clinical benchmarks, we also include unsupervised baselines developed for variant effect prediction in humans, such as SIFT [Ng and Henikoff, 2002], MutPred [Li et al., 2009], LRT [Chun and Fay, 2009], MutationAssessor [Reva et al., 2011], PROVEAN [Choi et al., 2012], PrimateAI [Sundaram et al., 2018] and LIST-S2 [Malhis et al., 2020].

4.2 Supervised benchmarks

DMS assays We leverage the same set of 250+ substitutions and indels DMS assays as for the zero-shot setting. In the supervised setting, greater care should be dedicated to mitigating overfitting risks, as the observations in biological datasets may not be fully independent. For instance, two mutations involving amino acids with similar biochemical properties at the same position will tend to produce similar effects. If we train on one of these mutations and test on the other, we will tend to overestimate our ability to predict the effects of mutants at unseen positions. In order to quantify the ability of each model to extrapolate to unseen positions at training time, we leverage 3 types of cross validation schemes introduced in Notin et al. [2023]. In the *Random* scheme, each mutation is randomly assigned to one of five different folds. In the *Contiguous* scheme, we split the sequence contiguously along its length, in order to obtain 5 segments of contiguous positions, and assign mutations to each segment based on the position at which it occurs. Lastly, in the *Modulo* scheme, we assign positions to each fold using the modulo operator to obtain 5 folds overall. In all supervised settings, we report both the Spearman’s rank correlation and Mean Squared Error (MSE) between predictions and experimental measurements. A more challenging generalization task would involve learning the relationship between protein representation (sequence, structure, or both) and function using only a handful of proteins, and then extrapolating at inference time to protein families not encountered during training. This setting may be seen as a hybrid between the zero-shot and supervised regimes – closer to zero-shot if we seek to predict different properties across families, and closer to the supervised setting if the properties are similar (eg., predicting the thermostability of proteins with low sequence similarity with the ones in the training set). While this study does not delve into these hybrid scenarios, the DMS assays in ProteinGym can facilitate such analyses.

Clinical datasets Given the restrictions on the number of labels available per gene and the discrepancies between train-validation-test splits across the different supervised baselines, we report test performance on the full set of all available ClinVar labels. We note that this may result in overestimating the performance of supervised methods for which the training data would substantially overlap with the labels considered in our ClinVar set. Further data leakage occurs for models trained on population frequencies, as most ClinVar benign labels are established based on observed frequencies in humans (situation especially evident for our indel dataset where we use frequent variants as pseudocontrols). Interestingly, despite this overfitting risk and as first observed in Frazer et al. [2021], we find that most supervised methods are outperformed by the best unsupervised methods (Fig. 2).

Baselines For the supervised DMS benchmark, we report two suites of baselines. The first suite is comprised of models that take as inputs One-Hot-Encoded (OHE) features. Following the protocol described in Hsu et al. [2022a], we augment the model inputs with predictions from several state-of-the-art zero-shot baselines: DeepSequence [Riesselman et al., 2018], ESM-1v [Meier et al., 2021], MSA Transformer [Rao et al., 2019], Tranception [Notin et al., 2022a] and TranceptEVE [Notin et al., 2022b]. Following prior works from the semi-supervised protein modeling literature [Heinzinger et al., 2019, Dallago et al., 2021], the second suite is formed with baselines that leverage mean-pooled embeddings from several protein language models (ESM-1v, MSA Transformer and Tranception) in lieu of OHE features. We also augment these baselines with zero-shot predictions obtained with the same model used to extract the protein sequence embeddings. Lastly, we include ProteinNPT [Notin et al., 2023], a semi-supervised pseudo-generative architecture which jointly models sequences and labels by performing axial attention [Ho et al., 2019b, Kossen et al., 2022] on input labeled batches. Additional details for the corresponding model architectures are reported in Appendix A.4.2. On the various clinical benchmarks, the above baselines are challenging to train given the low number of labels available per gene. We instead include several supervised baselines that have been specifically developed for variant effects predictions in humans, such as ClinPred [Alirezaie et al., 2018], MetaRNN [Li et al., 2022], BayesDel [Feng, 2017], REVEL [Ioannidis et al., 2016] and PolyPhen-2 [Adzhubei et al., 2010] (full list in A.4.3).

5 Results

5.1 Substitution benchmarks

We follow the experimental protocol described in § 4.1 and report our main results on the zero-shot DMS benchmarks in Table 2, supervised DMS benchmark in Table 3, and combined supervised and unsupervised clinical benchmarks in Fig. 2A. TranceptEVE emerges as the best overall method across the various settings. One of the key objectives of ProteinGym benchmarks is to analyze performance across a wide range of regimes to guide model selection depending on the objectives of the practitioners. To that end we also provide a performance breakdown across MSA depth, mutational depth and taxa where relevant (see Appendix A.5 and supplements). While TranceptEVE tops the ranking across the majority of metrics and settings, GEMME achieves the best performance in several categories, such as assays of viral or non-human eukaryotic proteins, and low and medium depth MSAs. While we report average performance per metric in Table 2, the *distribution* of scores across assays is also insightful. For instance, certain models are heavily penalized in aggregate rankings due to very poor performance on a handful of assays (e.g., ESM-1v), such that looking at the median performance in lieu of the average provides a complementary viewpoint. Furthermore, although most models rank similarly under Spearman and NDCG, some have comparatively better performance in one over the other (Fig. 2B). Superior ranking under NDCG may suggest a model is better at predicting the top end of a score distribution, which may be a desirable feature when using models for design and optimization. Many of the alignment-based methods (e.g. EVmutation, WaveNet and DeepSequence) exhibit this behavior (Fig. A1). Models with higher relative Spearman (e.g., ESM-1v and ESM-2) may be more effective for cases where the model needs to learn the full property distribution well, such as with mutation effect prediction. Lastly, in the zero-shot setting, autoregressive protein language models (e.g., Tranception, ProGen2) tend to outperform their masked language modeling (MLM) counterparts (e.g., ESM models). However, in supervised settings, both types of models provide valuable embeddings for learning. The optimal method depends on the specific situation, as observed in Table 3 and Table A16. The best performance is achieved with the ProteinNPT architecture, demonstrating the value from performing self-attention alternatively across columns (i.e., amino acid tokens and labels) and rows (i.e., protein sequences) to learn a rich representation of the data.

5.2 Indel benchmarks

The results for an indel-compatible subset of the models in ProteinGym is shown in Table 4. The Spearman rank correlations are separated by the method used to generate test sequences: unbiased libraries, or model-designed sequences biased towards natural sequences. The medium sized Tranception model has the highest Spearman rank correlation and AUC across all the assays, although TranceptEVE is the highest performing on the subset of assays measuring designed or natural sequences. We provide additional results on the clinical indel benchmarks in Appendix A.5.

Model type	Model name	Spearman	AUC	MCC	NDCG	Recall
Alignment-based	Site-Independent	0.361	0.697	0.288	0.746	0.201
	WaveNet	0.216	0.623	0.174	0.684	0.154
	EVmutation	0.397	0.717	0.306	0.775	0.220
	DeepSequence (ens.)	0.422	0.731	0.330	0.775	0.227
	EVE (ens.)	0.441	0.741	0.343	0.781	0.231
	GEMME	0.457	0.750	0.353	0.775	0.209
Protein language	UniRep	0.193	0.607	0.149	0.647	0.14
	CARP (640M)	0.373	0.704	0.289	0.749	0.210
	RITA XL	0.373	0.708	0.294	0.750	0.194
	ProGen2 XL	0.392	0.718	0.307	0.766	0.200
	ESM-1b	0.399	0.722	0.315	0.748	0.205
	ESM2 (15B)	0.405	0.723	0.318	0.759	0.210
	ESM-1v (ens.)	0.416	0.730	0.329	0.753	0.216
	VESPA	0.437	0.743	0.348	0.774	0.201
Hybrid	UniRep evotuned	0.347	0.693	0.274	0.737	0.181
	MSA Transformer (ens.)	0.434	0.738	0.341	0.777	0.224
	Tranception L	0.436	0.740	0.342	0.778	0.221
	TranceptEVE L	0.457	0.752	0.357	0.785	0.231
Inverse Folding	ProteinMPNN	0.258	0.640	0.196	0.712	0.186
	MIF-ST	0.401	0.718	0.310	0.766	0.227
	ESM-IF1	0.422	0.730	0.331	0.748	0.223

Table 2: **Zero-shot substitution DMS benchmark** Average Spearman’s rank correlation, AUC, MCC, NDCG@10%, and top 10% recall between model scores and experimental measurements on the ProteinGym substitution benchmark. We use ‘ens.’ as a shorthand for ensemble.

Model type	Model name	Spearman (↑)				MSE (↓)			
		Contig.	Mod.	Rand.	Avg.	Contig.	Mod.	Rand.	Avg.
OHE	None	0.064	0.027	0.579	0.224	1.158	1.125	0.898	1.061
	DeepSequence	0.400	0.400	0.521	0.440	0.967	0.940	0.767	0.891
	ESM-1v	0.367	0.368	0.514	0.417	0.977	0.949	0.764	0.897
	MSAT	0.410	0.412	0.536	0.453	0.963	0.934	0.749	0.882
	Tranception	0.419	0.419	0.535	0.458	0.985	0.934	0.766	0.895
	TranceptEVE	0.441	0.440	0.550	0.477	0.953	0.914	0.743	0.870
Embed.	ESM-1v	0.481	0.506	0.639	0.542	0.937	0.861	0.563	0.787
	MSAT	0.525	0.538	0.642	0.568	0.836	0.795	0.573	0.735
	Tranception	0.490	0.526	0.696	0.571	0.972	0.833	0.503	0.769
NPT	ProteinNPT	0.547	0.564	0.730	0.613	0.820	0.771	0.459	0.683

Table 3: **Supervised substitution DMS benchmark**. Spearman’s rank correlation and MSE between model predictions and experimental measurements. MSAT is a shorthand for MSA Transformer.

6 Resources

Codebase A key contribution of our work is the consolidation of the numerous baselines discussed in § 4 in a single open-source GitHub repository. While the main code for the majority of these baselines is publicly available, it often does not support fitness prediction out-of-the-box or, when it does, the codebase does not necessarily provide all the required data processing logic (e.g., pre-processing of MSAs in MSA Transformer) or handle all possible edge cases that may be encountered (e.g., scoring of sequences longer than context size in the ESM suite). Our GitHub repository addresses all of these gaps and provides a consistent interface that will aid in the seamless integration of new baselines as they become available.

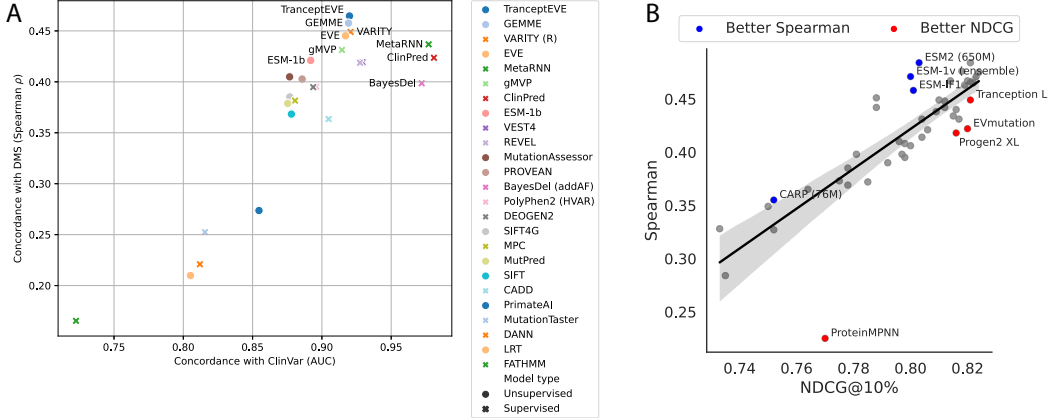


Figure 2: **Comparing baselines across datasets and across performance metrics** (A) Performance estimated against known clinical labels (avg. AUC over genes in ClinVar (x axis)), and DMS assays assessing the clinical effect of variants in humans (avg. Spearman (y axis)). (B) The zero-shot models’ median NDCG@10% (x-axis) against median Spearman (y-axis) on the DMS substitutions.

Model type	Model name	Spearman by DMS type (↑)		AUC (↑)	
		Library	Designed/Natural	All	All
Alignment models	HMM	0.459	0.385	0.391	0.731
	WaveNet	0.427	0.289	0.285	0.667
Protein language models	UniRep	-0.016	0.159	0.169	0.589
	RITA L	0.395	0.521	0.459	0.764
	ProtGPT2	0.153	0.188	0.194	0.615
	ProGen2 XL	0.369	0.471	0.434	0.749
Hybrid models	Tranception L	0.449	0.443	0.399	0.742
	Tranception M	0.529	0.392	0.298	0.735
	TranceptEVE	0.472	0.521	0.457	0.774

Table 4: **Zero-shot indel DMS benchmark** Spearman’s rank correlations and AUC between model scores and experimental measurements.

Processed datasets We also make publicly available all processed datasets used in our various benchmarks in a consistent format, including all DMS assays, model scores, ClinVar/gnomAD datasets, predicted 3D structures and Multiple Sequence Alignments required for training and scoring (see Section A.3.3 for more details).

Website Lastly, we developed a user-friendly website in which all benchmarks are accessible, with functionalities to support drill analyses across various dimensions (e.g., mutational depth, taxa) and exporting capabilities.

7 Conclusion

ProteinGym addresses the lack of large-scale benchmarks for the robust assessment of models developed for protein design and fitness prediction. It facilitates the direct comparison of methods across several dimensions of interest (e.g., MSA depth, mutational depth, taxa), based on different ground truth datasets (e.g., DMS assays vs Clinical annotations), and in different regimes (e.g., zero-shot vs supervised). We expect the ProteinGym benchmarks and the various data assets we publicly release along with them, to be valuable resources for the Machine Learning and Computational Biology communities, and we plan to continue updating the benchmarks as new assays and baselines become available.

Acknowledgments and Disclosure of Funding

P.N. was supported by GSK and the UK Engineering and Physical Sciences Research Council (ESPRC ICASE award no.18000077). Y.G. holds a Turing AI Fellowship (Phase 1) at the Alan Turing Institute, which is supported by EPSRC grant reference V030302/1. A.K., P.N., and D.S.M. are supported by a Chan Zuckerberg Initiative Award (Neurodegeneration Challenge Network, CZI2018-191853). S.P., H.S., and D.S.M. are supported by a NIH Transformational Research Award (TR01 1R01CA260415). L.v.N. and R.O. gratefully acknowledge funding from CZI NDCN. R.W. is supported by the UK Engineering and Physical Sciences Research Council, as part of the CDT in Health Data Science. D.F is supported by Wellcome Leap Inc, Chan Zuckerberg Initiative/Silicon Valley Community Foundation and The Coalition for Epidemic Preparedness Innovations. We thank the broader Marks Lab, in particular Javier Marchena-Hurtado, for helpful discussions when writing this manuscript. We gratefully acknowledge the compute resources provided by Invitae to train most of the EVE models that we used for the clinical benchmark.

References

Christopher D. Aakre, Julien Herrou, Tuyen N. Phung, Barrett S. Perchuk, Sean Crosson, and Michael T. Laub. Evolving New Protein-Protein Interaction Specificity through Promiscuous Intermediates. *Cell*, 163(3):594–606, October 2015. ISSN 00928674. doi: 10.1016/j.cell.2015.09.055. URL <https://linkinghub.elsevier.com/retrieve/pii/S0092867415012726>.

Bharat V. Adkar, Arti Tripathi, Anusmita Sahoo, Kanika Bajaj, Devrishi Goswami, Purbani Chakrabarti, Mohit K. Swarnkar, Rajesh S. Gokhale, and Raghavan Varadarajan. Protein Model Discrimination Using Mutational Sensitivity Derived from Deep Sequencing. *Structure*, 20(2):371–381, February 2012. ISSN 09692126. doi: 10.1016/j.str.2011.11.021. URL <https://linkinghub.elsevier.com/retrieve/pii/S0969212612000068>.

Ivan A Adzhubei, Steffen Schmidt, Leonid Peshkin, Vasily E Ramensky, Anna Gerasimova, Peer Bork, Alexey S Kondrashov, and Shamil R Sunyaev. A method and server for predicting damaging missense mutations. *Nature Methods*, 7(4):248–249, April 2010. ISSN 1548-7091, 1548-7105. doi: 10.1038/nmeth0410-248. URL <http://www.nature.com/articles/nmeth0410-248>.

Ethan Ahler, Ames C. Register, Sujata Chakraborty, Linglan Fang, Emily M. Dieter, Katherine A. Sitko, Rama Subba Rao Vidadala, Bridget M. Trevillian, Martin Golkowski, Hannah Gelman, Jason J. Stephany, Alan F. Rubin, Ethan A. Merritt, Douglas M. Fowler, and Dustin J. Maly. A Combined Approach Reveals a Regulatory Mechanism Coupling Src’s Kinase Activity, Localization, and Phosphotransferase-Independent Functions. *Molecular Cell*, 74(2):393–408.e20, April 2019. ISSN 10972765. doi: 10.1016/j.molcel.2019.02.003. URL <https://linkinghub.elsevier.com/retrieve/pii/S1097276519300930>.

Najmeh Alirezaie, Kristin D Kernohan, Taila Hartley, Jacek Majewski, and Toby Dylan Hocking. Clinpred: prediction tool to identify disease-relevant nonsynonymous single-nucleotide variants. *The American Journal of Human Genetics*, 103(4):474–483, 2018.

Ethan C. Alley, Grigory Khimulya, Surojit Biswas, Mohammed AlQuraishi, and George M. Church. Unified rational protein engineering with sequence-based deep representation learning. *Nature Methods*, pages 1–8, 2019a.

Ethan C Alley, Grigory Khimulya, Surojit Biswas, Mohammed AlQuraishi, and George M Church. Unified rational protein engineering with sequence-based deep representation learning. *Nature methods*, 16(12):1315–1322, 2019b.

Clara J. Amorosi, Melissa A. Chiasson, Matthew G. McDonald, Lai Hong Wong, Katherine A. Sitko, Gabriel Boyle, John P. Kowalski, Allan E. Rettie, Douglas M. Fowler, and Maitreya J. Dunham. Massively parallel characterization of CYP2C9 variant enzyme activity and abundance. *The American Journal of Human Genetics*, 108(9):1735–1751, September 2021. ISSN 00029297. doi: 10.1016/j.ajhg.2021.07.001. URL <https://linkinghub.elsevier.com/retrieve/pii/S000292972100269X>.

Bryan Andrews and Stanley Fields. Distinct patterns of mutational sensitivity for λ resistance and maltodextrin transport in *Escherichia coli* LamB. *Microbial Genomics*, 6(4), April 2020.

Carlos L. Araya, Douglas M. Fowler, Wentao Chen, Ike Muniez, Jeffery W. Kelly, and Stanley Fields. A fundamental protein property, thermodynamic stability, revealed solely from large-scale measurements of protein function. *Proceedings of the National Academy of Sciences*, 109(42):16858–16863, October 2012. ISSN 0027-8424, 1091-6490. doi: 10.1073/pnas.1209751109. URL <https://pnas.org/doi/full/10.1073/pnas.1209751109>.

Pradeep Bandaru, Neel H Shah, Moitrayee Bhattacharyya, John P Barton, Yasushi Kondo, Joshua C Cofsky, Christine L Gee, Arup K Chakraborty, Tanja Kortemme, Rama Ranganathan, and John Kuriyan. Deconstruction of the Ras switching cycle through saturation mutagenesis. *eLife*, 6:e27810, July 2017. ISSN 2050-084X. doi: 10.7554/eLife.27810. URL <https://elifesciences.org/articles/27810>.

Jesse D Bloom. An experimentally determined evolutionary model dramatically improves phylogenetic fit. *Molecular Biology and Evolution*, 31(8):1956–1978, August 2014.

Benedetta Bolognesi, Andre J. Faure, Mireia Seuma, Jörn M. Schmiedel, Gian Gaetano Tartaglia, and Ben Lehner. The mutational landscape of a prion-like domain. *Nature Communications*, 10(1):4162, December 2019. ISSN 2041-1723. doi: 10.1038/s41467-019-12101-z. URL <http://www.nature.com/articles/s41467-019-12101-z>.

Jeffrey I Boucher, Daniel NA Bolon, and Dan S Tawfik. Quantifying and understanding the fitness effects of protein mutations: Laboratory versus nature. *Protein Science*, 25(7):1219–1226, 2016.

Nadav Brandes and Vasilis Ntranos. ESM variants - data & code for analysis and figures, June 2023. URL <https://doi.org/10.5281/zenodo.8088402>.

Nadav Brandes, Grant Goldman, Charlotte H Wang, Chun Jimmie Ye, and Vasilis Ntranos. Genome-wide prediction of disease variant effects with a deep protein language model. *Nature Genetics*, 55(9):1512–1522, 2023.

Lisa Brenan, Aleksandr Andreev, Ofir Cohen, Sasha Pantel, Atanas Kamburov, Davide Cacchiarelli, Nicole S. Persky, Cong Zhu, Mukta Bagul, Eva M. Goetz, Alex B. Burgin, Levi A. Garraway, Gad Getz, Tarjei S. Mikkelsen, Federica Piccioni, David E. Root, and Cory M. Johannessen. Phenotypic Characterization of a Comprehensive Set of MAPK1 /ERK2 Missense Mutants. *Cell Reports*, 17(4):1171–1183, October 2016. ISSN 22111247. doi: 10.1016/j.celrep.2016.09.061. URL <https://linkinghub.elsevier.com/retrieve/pii/S2211124716313171>.

Jessica L. Bridgford, Su Min Lee, Christine M. M. Lee, Paola Guglielmelli, Elisa Rumi, Daniela Pietra, Stephen Wilcox, Yash Chhabra, Alan F. Rubin, Mario Cazzola, Alessandro M. Vannucchi, Andrew J. Brooks, Matthew E. Call, and Melissa J. Call. Novel drivers and modifiers of MPL-dependent oncogenic transformation identified by deep mutational scanning. *Blood*, 135(4):287–292, January 2020. ISSN 0006-4971, 1528-0020. doi: 10.1182/blood.2019002561. URL <https://ashpublications.org/blood/article/135/4/287/381157/Novel-drivers-and-modifiers-of-MPLdependent>.

Ian J Campbell, Joshua T Atkinson, Matthew D Carpenter, Dru Myerscough, Lin Su, Caroline M Ajo-Franklin, and Jonathan J Silberg. Determinants of multiheme cytochrome extracellular electron transfer uncovered by systematic peptide insertion. *Biochemistry*, 61(13):1337–1350, July 2022.

Henriette Capel, Robin Weiler, Maurits Dijkstra, Reinier Vleugels, Peter Bloem, and K. Anton Feenstra. ProteinGLUE multi-task benchmark suite for self-supervised protein modeling. *Scientific Reports*, 12(1):16047, September 2022. ISSN 2045-2322. doi: 10.1038/s41598-022-19608-4. URL <https://www.nature.com/articles/s41598-022-19608-4>. Number: 1 Publisher: Nature Publishing Group.

Hannah Carter, Christopher Douville, Peter D Stenson, David N Cooper, and Rachel Karchin. Identifying mendelian disease genes with the variant effect scoring tool. *BMC genomics*, 14(3):1–16, 2013.

Sujata Chakraborty, Ethan Ahler, Jessica J Simon, Linglan Fang, Zachary E Potter, Katherine A Sitko, Jason J Stephany, Miklos Guttman, Douglas M Fowler, and Dustin J Maly. Profiling of the drug resistance of thousands of src tyrosine kinase mutants uncovers a regulatory network that couples autoinhibition to catalytic domain dynamics. December 2021.

Kui K. Chan, Danielle Dorosky, Preeti Sharma, Shawn A. Abbasi, John M. Dye, David M. Kranz, Andrew S. Herbert, and Erik Procko. Engineering human ACE2 to optimize binding to the spike protein of SARS coronavirus 2. *Science*, 369(6508):1261–1265, September 2020. ISSN 0036-8075, 1095-9203. doi: 10.1126/science.abc0870. URL <https://www.science.org/doi/10.1126/science.abc0870>.

Yvonne H. Chan, Sergey V. Venev, Konstantin B. Zeldovich, and C. Robert Matthews. Correlation of fitness landscapes from three orthologous TIM barrels originates from sequence and structure constraints. *Nature Communications*, 8(1):14614, April 2017. ISSN 2041-1723. doi: 10.1038/ncomms14614. URL <http://www.nature.com/articles/ncomms14614>.

John Z Chen, Douglas M Fowler, and Nobuhiko Tokuriki. Comprehensive exploration of the translocation, stability and substrate recognition requirements in VIM-2 lactamase. *eLife*, 9:e56707, June 2020. ISSN 2050-084X. doi: 10.7554/eLife.56707. URL <https://elifesciences.org/articles/56707>.

Tianlong Chen, Chengyue Gong, Daniel Jesus Diaz, Xuxi Chen, Jordan Tyler Wells, Qiang Liu, Zhangyang Wang, Andrew Ellington, Alex Dimakis, and Adam Klivans. HotProtein: A Novel Framework for Protein Thermostability Prediction and Editing. October 2022. URL https://openreview.net/forum?id=RtV_iEbWeGE.

Yongcan Chen, Ruyun Hu, Keyi Li, Yating Zhang, Lihao Fu, Jianzhi Zhang, and Tong Si. Deep mutational scanning of an Oxygen-Independent fluorescent protein CreiLOV for comprehensive profiling of mutational and epistatic effects. *ACS Synthetic Biology*, 12(5):1461–1473, May 2023.

Melissa A Chiasson, Nathan J Rollins, Jason J Stephany, Katherine A Sitko, Kenneth A Matreyek, Marta Verby, Song Sun, Frederick P Roth, Daniel DeSloover, Debora S Marks, Allan E Rettie, and Douglas M Fowler. Multiplexed measurement of variant abundance and activity reveals VKOR topology, active site and human variant impact. *eLife*, 9:e58026, September 2020. ISSN 2050-084X. doi: 10.7554/eLife.58026. URL <https://elifesciences.org/articles/58026>.

Yongwook Choi, Gregory E Sims, Sean Murphy, Jason R Miller, and Agnes P Chan. Predicting the functional effect of amino acid substitutions and indels. *PLoS One*, 7(10):e46688, October 2012.

Sung Chun and Justin C Fay. Identification of deleterious mutations within three human genomes. *Genome research*, 19(9):1553–1561, 2009.

Lene Clausen, Vasileios Voutsinos, Matteo Cagiada, Kristoffer E Johansson, Martin Grønbæk-Thygesen, Snehal Nariya, Rachel L Powell, Magnus K N Have, Vibe H Oestergaard, Amelie Stein, Douglas M Fowler, Kresten Lindorff-Larsen, and Rasmus Hartmann-Petersen. A mutational atlas for parkin proteostasis. June 2023.

Willow Coyote-Maestas, David Nedrud, Yungui He, and Daniel Schmidt. Determinants of trafficking, conduction, and disease within a K⁺ channel revealed through multiparametric deep mutational scanning. *eLife*, 11: e76903, May 2022. ISSN 2050-084X. doi: 10.7554/eLife.76903. URL <https://elifesciences.org/articles/76903>.

Christian Dallago, Jody Mou, Kadina E Johnston, Bruce J Wittmann, Nicholas Bhattacharya, Samuel Goldman, Ali Madani, and Kevin K Yang. FLIP: Benchmark tasks in fitness landscape inference for proteins. 2021.

Rohan Dandage, Rajesh Pandey, Gopal Jayaraj, Manish Rai, David Berger, and Kausik Chakraborty. Differential strengths of molecular determinants guide environment specific mutational fates. *PLOS Genetics*, 14(5): e1007419, May 2018. ISSN 1553-7404. doi: 10.1371/journal.pgen.1007419. URL <https://dx.plos.org/10.1371/journal.pgen.1007419>.

J Dauparas, I Anishchenko, N Bennett, H Bai, R J Ragotte, L F Milles, B I M Wicky, A Courbet, R J de Haas, N Bethel, P J Y Leung, T F Huddy, S Pellock, D Tischer, F Chan, B Koepnick, H Nguyen, A Kang, B Sankaran, A K Bera, N P King, and D Baker. Robust deep learning-based protein sequence design using ProteinMPNN. *Science*, 378(6615):49–56, October 2022.

Natalie L. Dawson, Tony E. Lewis, Sayoni Das, Jonathan G. Lees, David A. Lee, Paul Ashford, Christine A. Orengo, and Ian P. W. Sillitoe. Cath: an expanded resource to predict protein function through structure and sequence. *Nucleic Acids Research*, 45:D289 – D295, 2016. URL <https://api.semanticscholar.org/CorpusID:9356024>.

Zhifeng Deng, Wanzhi Huang, Erol Bakkalbasi, Nicholas G. Brown, Carolyn J. Adamski, Kacie Rice, Donna Muzny, Richard A. Gibbs, and Timothy Palzkill. Deep Sequencing of Systematic Combinatorial Libraries Reveals beta-Lactamase Sequence Constraints at High Resolution. *Journal of Molecular Biology*, 424(3-4): 150–167, December 2012. ISSN 00222836. doi: 10.1016/j.jmb.2012.09.014. URL <https://linkinghub.elsevier.com/retrieve/pii/S0022283612007711>.

Jacob Devlin, Ming-Wei Chang, Kenton Lee, and Kristina Toutanova. BERT: Pre-training of deep bidirectional transformers for language understanding, 2019.

David Ding, Ada Shaw, Sam Sinai, Nathan Rollins, Noam Prywes, David F Savage, Michael T Laub, and Debora S Marks. Protein design using structure-based residue preferences. June 2023.

Michael Doud and Jesse Bloom. Accurate Measurement of the Effects of All Amino-Acid Mutations on Influenza Hemagglutinin. *Viruses*, 8(6):155, June 2016. ISSN 1999-4915. doi: 10.3390/v8060155. URL <http://www.mdpi.com/1999-4915/8/6/155>.

Michael B. Doud, Orr Ashenberg, and Jesse D. Bloom. Site-Specific Amino Acid Preferences Are Mostly Conserved in Two Closely Related Protein Homologs. *Molecular Biology and Evolution*, 32(11):2944–2960, November 2015. ISSN 0737-4038, 1537-1719. doi: 10.1093/molbev/msv167. URL <https://academic.oup.com/mbe/article-lookup/doi/10.1093/molbev/msv167>.

Maria Duenas-Decamp, Li Jiang, Daniel Bolon, and Paul R. Clapham. Saturation Mutagenesis of the HIV-1 Envelope CD4 Binding Loop Reveals Residues Controlling Distinct Trimer Conformations. *PLOS Pathogens*, 12(11):e1005988, November 2016. ISSN 1553-7374. doi: 10.1371/journal.ppat.1005988. URL <https://dx.plos.org/10.1371/journal.ppat.1005988>.

Richard Durbin, Sean Eddy, Anders Krogh, and Graeme Mitchison. *Biological Sequence Analysis: Probabilistic Models of Proteins and Nucleic Acids*. Cambridge University Press, 1998.

Sean R Eddy. Accelerated profile HMM searches. *PLoS Comput. Biol.*, 7(10):e1002195, October 2011.

Assaf Elazar, Jonathan Weinstein, Ido Biran, Yearit Fridman, Eitan Bibi, and Sarel Jacob Fleishman. Mutational scanning reveals the determinants of protein insertion and association energetics in the plasma membrane. *eLife*, 5:e12125, January 2016. ISSN 2050-084X. doi: 10.7554/eLife.12125. URL <https://elifesciences.org/articles/12125>.

Ahmed Elnaggar, Michael Heinzinger, Christian Dallago, Ghalia Rehawi, Wang Yu, Llion Jones, Tom Gibbs, Tamas B. Fehér, Christoph Angerer, Martin Steinegger, Debsindhu Bhowmik, and Burkhard Rost. Prottrans: Towards cracking the language of life's code through self-supervised deep learning and high performance computing. *IEEE transactions on pattern analysis and machine intelligence*, PP, 2021.

Stefan Engelen, Ladislas A Trojan, Sophie Sacquin-Mora, Richard Lavery, and Alessandra Carbone. Joint evolutionary trees: a large-scale method to predict protein interfaces based on sequence sampling. *PLoS computational biology*, 5(1):e1000267, 2009.

Steven Erwood, Teija M. I. Bily, Jason Lequyer, Joyce Yan, Nitya Gulati, Reid A. Brewer, Liangchi Zhou, Laurence Pelletier, Evgueni A. Ivakine, and Ronald D. Cohn. Saturation variant interpretation using CRISPR prime editing. *Nature Biotechnology*, 40(6):885–895, June 2022. ISSN 1087-0156, 1546-1696. doi: 10.1038/s41587-021-01201-1. URL <https://www.nature.com/articles/s41587-021-01201-1>.

Gabriella O. Estevam, Edmond M. Linossi, Christian B. Macdonald, Carla A. Espinoza, Jennifer M. Michaud, Willow Coyote-Maestas, Eric A. Collisson, Natalia Jura, and James S. Fraser. Conserved regulatory motifs in the juxtamembrane domain and kinase N-lobe revealed through deep mutational scanning of the MET receptor tyrosine kinase domain. preprint, Molecular Biology, August 2023. URL <http://biorxiv.org/lookup/doi/10.1101/2023.08.03.551866>.

Andre J. Faure, Júlia Domingo, Jörn M. Schmiedel, Cristina Hidalgo-Carcedo, Guillaume Diss, and Ben Lehner. Mapping the energetic and allosteric landscapes of protein binding domains. *Nature*, 604(7904): 175–183, April 2022. ISSN 0028-0836, 1476-4687. doi: 10.1038/s41586-022-04586-4. URL <https://www.nature.com/articles/s41586-022-04586-4>.

Bing-Jian Feng. PERCH: a unified framework for disease gene prioritization. *Human mutation*, 38(3):243–251, 2017.

Jason D. Fernandes, Tyler B. Faust, Nicolas B. Strauli, Cynthia Smith, David C. Crosby, Robert L. Nakamura, Ryan D. Hernandez, and Alan D. Frankel. Functional Segregation of Overlapping Genes in HIV. *Cell*, 167(7):1762–1773.e12, December 2016. ISSN 00928674. doi: 10.1016/j.cell.2016.11.031. URL <https://linkinghub.elsevier.com/retrieve/pii/S0092867416316038>.

Noelia Ferruz, Steffen Schmidt, and Birte Höcker. ProtGPT2 is a deep unsupervised language model for protein design. *Nature Communications*, 13, 2022.

Gregory M. Findlay, Riza M. Daza, Beth Martin, Melissa D. Zhang, Anh P. Leith, Molly Gasperini, Joseph D. Janizek, Xingfan Huang, Lea M. Starita, and Jay Shendure. Accurate classification of BRCA1 variants with saturation genome editing. *Nature*, 562(7726):217–222, October 2018. ISSN 0028-0836, 1476-4687. doi: 10.1038/s41586-018-0461-z. URL <https://www.nature.com/articles/s41586-018-0461-z>.

Elad Firnberg, Jason W. Labonte, Jeffrey J. Gray, and Marc Ostermeier. A Comprehensive, High-Resolution Map of a Gene's Fitness Landscape. *Molecular Biology and Evolution*, 31(6):1581–1592, June 2014. ISSN 1537-1719, 0737-4038. doi: 10.1093/molbev/msu081. URL <https://academic.oup.com/mbe/article-lookup/doi/10.1093/molbev/msu081>.

Julia M Flynn, Ammeret Rossouw, Pamela Cote-Hammarlof, Inês Fragata, David Mavor, Carl Hollins, Claudia Bank, and Daniel Na Bolon. Comprehensive fitness maps of Hsp90 show widespread environmental dependence. *eLife*, 9:e53810, March 2020. ISSN 2050-084X. doi: 10.7554/eLife.53810. URL <https://elifesciences.org/articles/53810>.

Julia M. Flynn, Neha Samant, Gily Schneider-Nachum, David T. Barkan, Nese Kurt Yilmaz, Celia A. Schiffer, Stephanie A. Moquin, Dustin Dovala, and Daniel N.A. Bolon. Comprehensive fitness landscape of SARS-CoV-2 M^{Pro} reveals insights into viral resistance mechanisms. preprint, Molecular Biology, January 2022. URL <http://biorxiv.org/lookup/doi/10.1101/2022.01.26.477860>.

Jonathan Frazer, Pascal Notin, Mafalda Dias, Aidan Gomez, Joseph K Min, Kelly P. Brock, Yarin Gal, and Debora S. Marks. Disease variant prediction with deep generative models of evolutionary data. *Nature*, 2021.

Kiran S Gajula, Peter J Huwe, Charlie Y Mo, Daniel J Crawford, James T Stivers, Ravi Radhakrishnan, and Rahul M Kohli. High-throughput mutagenesis reveals functional determinants for DNA targeting by activation-induced deaminase. *Nucleic Acids Research*, 42(15):9964–9975, September 2014.

Zhangyang Gao, Cheng Tan, and Stan Z. Li. Pifold: Toward effective and efficient protein inverse folding. *ArXiv*, abs/2209.12643, 2022. URL <https://api.semanticscholar.org/CorpusID:252596302>.

Sarah Gersing, Matteo Cagiada, Marinella Gebbia, Anette P. Gjesing, Atina G. Coté, Gireesh Seesankar, Roujia Li, Daniel Tabet, Amelie Stein, Anna L. Gloyn, Torben Hansen, Frederick P. Roth, Kresten Lindorff-Larsen, and Rasmus Hartmann-Petersen. A comprehensive map of human glucokinase variant activity. preprint, Genetics, May 2022. URL <http://biorxiv.org/lookup/doi/10.1101/2022.05.04.490571>.

Sarah Gersing, Thea K Schulze, Matteo Cagiada, Amelie Stein, Frederick P Roth, Kresten Lindorff-Larsen, and Rasmus Hartmann-Petersen. Characterizing glucokinase variant mechanisms using a multiplexed abundance assay. *bioRxiv*, May 2023.

Dia A Ghose, Kaitlyn E Przydzial, Emily M Mahoney, Amy E Keating, and Michael T Laub. Marginal specificity in protein interactions constrains evolution of a paralogous family. *Proceedings of the National Academy of Sciences of the United States of America*, 120(18):e2221163120, May 2023.

Andrew O. Giacomelli, Xiaoping Yang, Robert E. Lintner, James M. McFarland, Marc Duby, Jaegil Kim, Thomas P. Howard, David Y. Takeda, Seav Huong Ly, Eejung Kim, Hugh S. Gannon, Brian Hurlhula, Ted Sharpe, Amy Goodale, Briana Fritchman, Scott Steelman, Francisca Vazquez, Aviad Tsherniak, Andrew J. Aguirre, John G. Doench, Federica Piccioni, Charles W. M. Roberts, Matthew Meyerson, Gad Getz, Cory M. Johannessen, David E. Root, and William C. Hahn. Mutational processes shape the landscape of TP53 mutations in human cancer. *Nature Genetics*, 50(10):1381–1387, October 2018. ISSN 1061-4036, 1546-1718. doi: 10.1038/s41588-018-0204-y. URL <https://www.nature.com/articles/s41588-018-0204-y>.

Kevin S Gill, Kritika Mehta, Jeremiah D Heredia, Vishnu V Krishnamurthy, Kai Zhang, and Erik Procko. Multiple mechanisms of self-association of chemokine receptors CXCR4 and CCR5 demonstrated by deep mutagenesis. *bioRxiv*, March 2023.

Andrew M. Glazer, Brett M. Kroncke, Kenneth A. Matreyek, Tao Yang, Yuko Wada, Tiffany Shields, Joe-Elie Salem, Douglas M. Fowler, and Dan M. Roden. Deep Mutational Scan of an SCN5A Voltage Sensor. *Circulation: Genomic and Precision Medicine*, 13(1):e002786, February 2020. ISSN 2574-8300. doi: 10.1161/CIRCGEN.119.002786. URL <https://www.ahajournals.org/doi/10.1161/CIRCGEN.119.002786>.

Courtney E. Gonzalez, Paul Roberts, and Marc Ostermeier. Fitness Effects of Single Amino Acid Insertions and Deletions in TEM-1 beta-Lactamase. *Journal of Molecular Biology*, 431(12):2320–2330, May 2019. ISSN 00222836. doi: 10.1016/j.jmb.2019.04.030. URL <https://linkinghub.elsevier.com/retrieve/pii/S0022283619302372>.

Louisa Gonzalez Somermeyer, Aubin Fleiss, Alexander S Mishin, Nina G Bozhanova, Anna A Igolkina, Jens Meiler, Maria-Elisenda Alaball Pujol, Ekaterina V Putintseva, Karen S Sarkisyan, and Fyodor A Kondrashov. Heterogeneity of the GFP fitness landscape and data-driven protein design. *eLife*, 11:e75842, May 2022. ISSN 2050-084X. doi: 10.7554/eLife.75842. URL <https://elifesciences.org/articles/75842>.

Vanessa E Gray, Katherine Sitko, Floriane Z Ngako Kameni, Miriam Williamson, Jason J Stephany, Nicholas Hasle, and Douglas M Fowler. Elucidating the molecular determinants of A β aggregation with deep mutational scanning. *G3*, 9(11):3683–3689, November 2019.

Dominik G Grimm, Chloé-Agathe Azencott, Fabian Aicheler, Udo Gieraths, Daniel G MacArthur, Kaitlin E Samocha, David N Cooper, Peter D Stenson, Mark J Daly, Jordan W Smoller, Laramie E Duncan, and Karsten M Borgwardt. The evaluation of tools used to predict the impact of missense variants is hindered by two types of circularity. *Hum. Mutat.*, 36(5):513–523, May 2015.

Hugh K Haddox, Adam S Dingens, Sarah K Hilton, Julie Overbaugh, and Jesse D Bloom. Mapping mutational effects along the evolutionary landscape of HIV envelope. *eLife*, 7:e34420, March 2018. ISSN 2050-084X. doi: 10.7554/eLife.34420. URL <https://elifesciences.org/articles/34420>.

Michael Heinzinger, Ahmed Elnaggar, Yu Wang, Christian Dallago, Dmitrii Nechaev, Florian Matthes, and Burkhard Rost. Modeling aspects of the language of life through transfer-learning protein sequences. *BMC Bioinformatics*, 20(1):723, December 2019. ISSN 1471-2105. doi: 10.1186/s12859-019-3220-8. URL <https://doi.org/10.1186/s12859-019-3220-8>.

Daniel Hesslow, N. ed. Zanichelli, Pascal Notin, Iacopo Poli, and Debora S. Marks. RITA: a study on scaling up generative protein sequence models. *ArXiv*, abs/2205.05789, 2022.

Ryan T Hietpas, Jeffrey D Jensen, and Daniel N A Bolon. Experimental illumination of a fitness landscape. *Proceedings of the National Academy of Sciences of the United States of America*, 108(19):7896–7901, May 2011.

Jonathan Ho, Nal Kalchbrenner, Dirk Weissenborn, and Tim Salimans. Axial attention in multidimensional transformers. *ArXiv*, abs/1912.12180, 2019a. URL <https://api.semanticscholar.org/CorpusID:209323787>.

Jonathan Ho, Nal Kalchbrenner, Dirk Weissenborn, and Tim Salimans. Axial attention in multidimensional transformers. *arXiv preprint arXiv:1912.12180*, 2019b.

Helen T. Hobbs, Neel H. Shah, Sophie R. Shoemaker, Jeanine F. Amacher, Susan Marqusee, and John Kuriyan. Saturation mutagenesis of a predicted ancestral Syk-family kinase. *Protein Science*, 31(10), October 2022. ISSN 0961-8368, 1469-896X. doi: 10.1002/pro.4411. URL <https://onlinelibrary.wiley.com/doi/10.1002/pro.4411>.

Nancy Hom, Lauren Gentles, Jesse D Bloom, and Kelly K Lee. Deep mutational scan of the highly conserved influenza a virus M1 matrix protein reveals substantial intrinsic mutational tolerance. *Journal of Virology*, 93(13), July 2019.

Jirí Hon, Martin Marusiak, Tomáš Martínek, Antonín Kunka, Jaroslav Zendulka, David Bednář, and Jiří Damborský. SoluProt: prediction of soluble protein expression in escherichia coli. *Bioinformatics*, 37:23 – 28, 2020.

Thomas A Hopf, John B Ingraham, Frank J Poelwijk, Charlotta PI Schärfe, Michael Springer, Chris Sander, and Debora S Marks. Mutation effects predicted from sequence co-variation. *Nature biotechnology*, 35(2):128–135, 2017.

Chloe Hsu, Hunter Nisonoff, Clara Fannjiang, and Jennifer Listgarten. Learning protein fitness models from evolutionary and assay-labeled data. *Nature Biotechnology*, 40(7):1114–1122, July 2022a. ISSN 1087-0156, 1546-1696. doi: 10.1038/s41587-021-01146-5. URL <https://www.nature.com/articles/s41587-021-01146-5>.

Chloe Hsu, Robert Verkuil, Jason Liu, Zeming Lin, Brian Hie, Tom Sercu, Adam Lerer, and Alexander Rives. Learning inverse folding from millions of predicted structures. April 2022b.

Po-Ssu Huang, Scott E. Boyken, and David Baker. The coming of age of de novo protein design. *Nature*, 537:320–327, 2016. URL <https://api.semanticscholar.org/CorpusID:205251398>.

Zachary M Hutteringer, Laura M Haynes, Andrew Yee, Colin A Kretz, Matthew L Holding, David R Siemieniak, Daniel A Lawrence, and David Ginsburg. Deep mutational scanning of the plasminogen activator inhibitor-1 functional landscape. *Scientific Reports*, 11(1):18827, September 2021.

John Ingraham, Vikas Garg, Regina Barzilay, and Tommi Jaakkola. Generative models for graph-based protein design. *Advances in neural information processing systems*, 32, 2019.

Nilah M Ioannidis, Joseph H Rothstein, Vikas Pejaver, Sumit Middha, Shannon K McDonnell, Saurabh Baheti, Anthony Musolf, Qing Li, Emily Holzinger, Danielle Karyadi, et al. REVEL: an ensemble method for predicting the pathogenicity of rare missense variants. *The American Journal of Human Genetics*, 99(4):877–885, 2016.

Hervé Jacquier, André Birgy, Hervé Le Nagard, Yves Mechulam, Emmanuelle Schmitt, Jérémie Glodt, Beatrice Bercot, Emmanuelle Petit, Julie Poulain, Guilène Barnaud, Pierre-Alexis Gros, and Olivier Tenaillon. Capturing the mutational landscape of the beta-lactamase TEM-1. *Proceedings of the National Academy of Sciences*, 110(32):13067–13072, August 2013. ISSN 0027-8424, 1091-6490. doi: 10.1073/pnas.1215206110. URL <https://pnas.org/doi/full/10.1073/pnas.1215206110>.

Milind Jagota, Chengzhong Ye, Ruchir Rastogi, Carlos Albors, Antoine Kochl, Nilah M. Ioannidis, and Yun S. Song. Cross-protein transfer learning substantially improves zero-shot prediction of disease variant effects. 2022. URL <https://api.semanticscholar.org/CorpusID:253628877>.

Xiaoyan Jia, Bala Bharathi Burugula, Victor Chen, Rosemary M. Lemons, Sajini Jayakody, Mariam Maksutova, and Jacob O. Kitzman. Massively parallel functional testing of MSH2 missense variants conferring Lynch syndrome risk. *The American Journal of Human Genetics*, 108(1):163–175, January 2021. ISSN 00029297. doi: 10.1016/j.ajhg.2020.12.003. URL <https://linkinghub.elsevier.com/retrieve/pii/S0002929720304390>.

Li Jiang, Ping Liu, Claudia Bank, Nicholas Renzette, Kristina Prachanronarong, Lutfu S. Yilmaz, Daniel R. Caffrey, Konstantin B. Zeldovich, Celia A. Schiffer, Timothy F. Kowalik, Jeffrey D. Jensen, Robert W. Finberg, Jennifer P. Wang, and Daniel N.A. Bolon. A Balance between Inhibitor Binding and Substrate Processing Confers Influenza Drug Resistance. *Journal of Molecular Biology*, 428(3):538–553, February 2016. ISSN 00222836. doi: 10.1016/j.jmb.2015.11.027. URL <https://linkinghub.elsevier.com/retrieve/pii/S0022283615006907>.

Rosanna Junchen Jiang. *Exhaustive Mapping of Missense Variation in Coronary Heart Disease-related Genes*. PhD thesis, University of Toronto, November 2019. URL <https://hdl.handle.net/1807/98076>.

Bowen Jing, Stephan Eismann, Patricia Suriana, Raphael J L Townshend, and Ron Dror. Learning from protein structure with geometric vector perceptrons. September 2020.

Eric M Jones, Nathan B Lubock, Aj Venkatakrishnan, Jeffrey Wang, Alex M Tseng, Joseph M Paggi, Naomi R Latorraca, Daniel Cancilla, Megan Satyadi, Jessica E Davis, M Madan Babu, Ron O Dror, and Sriram Kosuri. Structural and functional characterization of G protein-coupled receptors with deep mutational scanning. *eLife*, 9:e54895, October 2020. ISSN 2050-084X. doi: 10.7554/eLife.54895. URL <https://elifesciences.org/articles/54895>.

John Jumper, Richard Evans, Alexander Pritzel, Tim Green, Michael Figurnov, Olaf Ronneberger, Kathryn Tunyasuvunakool, Russ Bates, Augustin Žídek, Anna Potapenko, Alex Bridgland, Clemens Meyer, Simon A A Kohl, Andrew J Ballard, Andrew Cowie, Bernardino Romera-Paredes, Stanislav Nikolov, Rishabh Jain, Jonas Adler, Trevor Back, Stig Petersen, David Reiman, Ellen Clancy, Michal Zielinski, Martin Steinegger, Michalina Pacholska, Tamas Berghammer, Sebastian Bodenstein, David Silver, Oriol Vinyals, Andrew W Senior, Koray Kavukcuoglu, Pushmeet Kohli, and Demis Hassabis. Highly accurate protein structure prediction with AlphaFold. *Nature*, July 2021.

Konrad J Karczewski, Laurent C Francioli, Grace Tiao, Beryl B Cummings, Jessica Alföldi, Qingbo Wang, Ryan L Collins, Kristen M Laricchia, Andrea Ganna, Daniel P Birnbaum, Laura D Gauthier, Harrison Brand, Matthew Solomonson, Nicholas A Watts, Daniel Rhodes, Moriel Singer-Berk, Eleina M England, Eleanor G Seaby, Jack A Kosmicki, Raymond K Walters, Katherine Tashman, Yossi Farjoun, Eric Banks, Timothy Poterba, Arcturus Wang, Cotton Seed, Nicola Whiffin, Jessica X Chong, Kaitlin E Samocha, Emma Pierce-Hoffman, Zachary Zappala, Anne H O'Donnell-Luria, Eric Vallabh Minikel, Ben Weisburd, Monkol Lek, James S Ware, Christopher Vittal, Irina M Armean, Louis Bergelson, Kristian Cibulskis, Kristen M Connolly, Miguel Covarrubias, Stacey Donnelly, Steven Ferriera, Stacey Gabriel, Jeff Gentry, Namrata Gupta, Thibault Jeandet, Diane Kaplan, Christopher Llanwarne, Ruchi Munshi, Sam Novod, Nikelle Petrillo, David Roazen, Valentin Ruano-Rubio, Andrea Saltzman, Molly Schleicher, Jose Soto, Kathleen Tibbetts, Charlotte Tolonen, Gordon Wade, Michael E Talkowski, Genome Aggregation Database Consortium, Benjamin M Neale, Mark J Daly, and Daniel G MacArthur. The mutational constraint spectrum quantified from variation in 141,456 humans. *Nature*, 581(7809):434–443, May 2020.

Eric D. Kelsic, Hattie Chung, Niv Cohen, Jimin Park, Harris H. Wang, and Roy Kishony. RNA Structural Determinants of Optimal Codons Revealed by MAGE-Seq. *Cell Systems*, 3(6):563–571.e6, December 2016. ISSN 24054712. doi: 10.1016/j.cels.2016.11.004. URL <https://linkinghub.elsevier.com/retrieve/pii/S2405471216303684>.

Paul Kennouche, Arthur Charles-Orszag, Daiki Nishiguchi, Sylvie Goussard, Anne-Flore Imhaus, Mathieu Dupré, Julia Chamot-Rooke, and Guillaume Duménil. Deep mutational scanning of the *Neisseria meningitidis* major pilin reveals the importance of pilus tip-mediated adhesion. *The EMBO Journal*, 38(22):e102145, November 2019. ISSN 0261-4189, 1460-2075. doi: 10.1525/embj.2019102145. URL <https://www.embopress.org/doi/10.1525/embj.2019102145>.

Jacob O Kitzman, Lea M Starita, Russell S Lo, Stanley Fields, and Jay Shendure. Massively parallel single-amino-acid mutagenesis. *Nature Methods*, 12(3):203–206, March 2015. ISSN 1548-7091, 1548-7105. doi: 10.1038/nmeth.3223. URL <http://www.nature.com/articles/nmeth.3223>.

Justin R. Klesmith, John-Paul Bacik, Ryszard Michalczyk, and Timothy A. Whitehead. Comprehensive Sequence-Flux Mapping of a Levoglucosan Utilization Pathway in *E. coli*. *ACS Synthetic Biology*, 4(11):1235–1243, November 2015. ISSN 2161-5063, 2161-5063. doi: 10.1021/acssynbio.5b00131. URL <https://pubs.acs.org/doi/10.1021/acssynbio.5b00131>.

Justin R. Klesmith, Lihe Su, Lan Wu, Ian A. Schrack, Fay J. Dufort, Alyssa Birt, Christine Ambrose, Benjamin J. Hackel, Roy R. Lobb, and Paul D. Rennert. Retargeting CD19 Chimeric Antigen Receptor T Cells via Engineered CD19-Fusion Proteins. *Molecular Pharmaceutics*, 16(8):3544–3558, August 2019. ISSN 1543-8384, 1543-8392. doi: 10.1021/acs.molpharmaceut.9b00418. URL <https://pubs.acs.org/doi/10.1021/acs.molpharmaceut.9b00418>.

Jannik Kossen, Neil Band, Clare Lyle, Aidan N. Gomez, Tom Rainforth, and Yarin Gal. Self-Attention Between Datapoints: Going Beyond Individual Input-Output Pairs in Deep Learning, February 2022. URL <http://arxiv.org/abs/2106.02584>. arXiv:2106.02584 [cs, stat] version: 2.

Eran Kotler, Odem Shani, Guy Goldfeld, Maya Lotan-Pompan, Ohad Tarcic, Anat Gershoni, Thomas A. Hopf, Debora S. Marks, Moshe Oren, and Eran Segal. A Systematic p53 Mutation Library Links Differential Functional Impact to Cancer Mutation Pattern and Evolutionary Conservation. *Molecular Cell*, 71(1):178–190.e8, July 2018. ISSN 10972765. doi: 10.1016/j.molcel.2018.06.012. URL <https://linkinghub.elsevier.com/retrieve/pii/S1097276518304544>.

Krystian A. Kozek, Andrew M. Glazer, Chai-Ann Ng, Daniel Blackwell, Christian L. Egly, Loren R. Vanags, Marcia Blair, Devyn Mitchell, Kenneth A. Matreyek, Douglas M. Fowler, Bjorn C. Knollmann, Jamie I. Vandenberg, Dan M. Roden, and Brett M. Kroncke. High-throughput discovery of trafficking-deficient variants in the cardiac potassium channel KV11.1. *Heart Rhythm*, 17(12):2180–2189, December 2020. ISSN 15475271. doi: 10.1016/j.hrthm.2020.05.041. URL <https://linkinghub.elsevier.com/retrieve/pii/S1547527120305427>.

Andriy Kryshtafovych, Torsten Schwede, Maya Topf, Krzysztof Fidelis, and John Moult. Critical assessment of methods of protein structure prediction (CASP)—Round XIV. *Proteins: Structure*, 89:1607 – 1617, 2021.

Jason J. Kwon, Behnoush Hajian, Yuemin Bian, Lucy C. Young, Alvaro J. Amor, James R. Fuller, Cara V. Fraley, Abbey M. Sykes, Jonathan So, Joshua Pan, Laura Baker, Sun Joo Lee, Douglas B. Wheeler, David L. Mayhew, Nicole S. Persky, Xiaoping Yang, David E. Root, Anthony M. Barsotti, Andrew W. Stamford, Charles K. Perry, Alex Burgin, Frank McCormick, Christopher T. Lemke, William C. Hahn, and Andrew J. Aguirre. Structure–function analysis of the SHOC2–MRAS–PP1C holophosphatase complex. *Nature*, 609(7926):408–415, September 2022. ISSN 0028-0836, 1476-4687. doi: 10.1038/s41586-022-04928-2. URL <https://www.nature.com/articles/s41586-022-04928-2>.

Elodie Laine, Yasaman Karami, and Alessandra Carbone. GEMME: A Simple and Fast Global Epistatic Model Predicting Mutational Effects. *Molecular Biology and Evolution*, 36(11):2604–2619, November 2019. ISSN 0737-4038. doi: 10.1093/molbev/msz179. URL <https://doi.org/10.1093/molbev/msz179>.

Melissa J. Landrum and Brandi L. Kattman. ClinVar at five years: Delivering on the promise. *Human Mutation*, 39(11):1623–1630, November 2018. ISSN 1098-1004. doi: 10.1002/humu.23641.

Juhye M. Lee, John Huddleston, Michael B. Doud, Kathryn A. Hooper, Nicholas C. Wu, Trevor Bedford, and Jesse D. Bloom. Deep mutational scanning of hemagglutinin helps predict evolutionary fates of human H3N2 influenza variants. *Proceedings of the National Academy of Sciences*, 115(35), August 2018. ISSN 0027-8424, 1091-6490. doi: 10.1073/pnas.1806133115. URL <https://pnas.org/doi/full/10.1073/pnas.1806133115>.

Ruipeng Lei, Andrea Hernandez Garcia, Timothy J C Tan, Qi Wen Teo, Yiquan Wang, Xiwen Zhang, Shitong Luo, Satish K Nair, Jian Peng, and Nicholas C Wu. Mutational fitness landscape of human influenza H3N2 neuraminidase. *Cell Reports*, 42(1):111951, January 2023.

Biao Li, Vidhya G Krishnan, Matthew E Mort, Fuxiao Xin, Kishore K Kamati, David N Cooper, Sean D Mooney, and Predrag Radivojac. Automated inference of molecular mechanisms of disease from amino acid substitutions. *Bioinformatics*, 25(21):2744–2750, 2009.

Chang Li, Degui Zhi, Kai Wang, and Xiaoming Liu. MetaRNN: differentiating rare pathogenic and rare benign missense SNVs and InDels using deep learning. *Genome Medicine*, 14(1):115, October 2022. ISSN 1756-994X. doi: 10.1186/s13073-022-01120-z. URL <https://genomemedicine.biomedcentral.com/articles/10.1186/s13073-022-01120-z>.

Yuan Li, Sarah Arcos, Kimberly R. Sabsay, Aartjan J.W. Te Velthuis, and Adam S. Lauring. Deep mutational scanning reveals the functional constraints and evolutionary potential of the influenza A virus PB1 protein. preprint, *Microbiology*, August 2023. URL <http://biorxiv.org/lookup/doi/10.1101/2023.08.27.554986>.

Zeming Lin, Halil Akin, Roshan Rao, Brian Hie, Zhongkai Zhu, Wenting Lu, Nikita Smetanin, Robert Verkuil, Ori Kabeli, Yaniv Shmueli, Allan dos Santos Costa, Maryam Fazel-Zarandi, Tom Sercu, Salvatore Candido, and Alexander Rives. Evolutionary-scale prediction of atomic-level protein structure with a language model. *Science*, 379(6637):1123–1130, March 2023. doi: 10.1126/science.ade2574.

Xiaoming Liu, Xueqiu Jian, and Eric Boerwinkle. dbnsfp: a lightweight database of human nonsynonymous snps and their functional predictions. *Human mutation*, 32(8):894–899, 2011.

Xiaoming Liu, Chang Li, Chengcheng Mou, Yibo Dong, and Yicheng Tu. dbnsfp v4: a comprehensive database of transcript-specific functional predictions and annotations for human nonsynonymous and splice-site snvs. *Genome medicine*, 12(1):1–8, 2020.

Benjamin J Livesey and Joseph A Marsh. Updated benchmarking of variant effect predictors using deep mutational scanning. *Molecular Systems Biology*, page e11474, 2023.

Russell S Lo, Gareth A Cromie, Michelle Tang, Kevin Teng, Katherine Owens, Amy Sirr, J Nathan Kutz, Hiroki Morizono, Ljubica Caldovic, Nicholas Ah Mew, Andrea Gropman, and Aimée M Dudley. The functional impact of 1,570 individual amino acid substitutions in human OTC. *American Journal of Human Genetics*, 110(5):863–879, May 2023.

Christian B. Macdonald, David Nedrud, Patrick Rockefeller Grimes, Donovan Trinidad, James S. Fraser, and Willow Coyote-Maestas. DIMPLE: deep insertion, deletion, and missense mutation libraries for exploring protein variation in evolution, disease, and biology. *Genome Biology*, 24(1):36, February 2023. ISSN 1474-760X. doi: 10.1186/s13059-023-02880-6. URL <https://genomebiology.biomedcentral.com/articles/10.1186/s13059-023-02880-6>.

Mark R MacRae, Dhenesh Puvanendran, Max A B Haase, Nicolas Coudray, Ljuvica Kolich, Cherry Lam, Minkyung Baek, Gira Bhabha, and Damian C Ekiert. Protein-protein interactions in the mla lipid transport system probed by computational structure prediction and deep mutational scanning. *Journal of Biological Chemistry*, 299(6):104744, June 2023.

Ali Madani, Bryan McCann, Nikhil Naik, Nitish Shirish Keskar, Namrata Anand, Raphael R. Eguchi, Po-Ssu Huang, and Richard Socher. ProGen: Language modeling for protein generation, 2020.

Nawar Malhis, Matthew Jacobson, Steven JM Jones, and Jörg Gsponer. LIST-S2: taxonomy based sorting of deleterious missense mutations across species. *Nucleic acids research*, 48(W1):W154–W161, 2020.

Céline Marquet, Michael Heinzinger, Tobias Olenyi, Christian Dallago, Kyra Erckert, Michael Bernhofer, Dmitrii Nechaev, and Burkhard Rost. Embeddings from protein language models predict conservation and variant effects. *Human Genetics*, 141(10):1629–1647, October 2022. ISSN 1432-1203. doi: 10.1007/s00439-021-02411-y.

Kenneth A. Matreyek, Lea M. Starita, Jason J. Stephany, Beth Martin, Melissa A. Chiasson, Vanessa E. Gray, Martin Kircher, Arineh Khechaduri, Jennifer N. Dines, Ronald J. Hause, Smita Bhatia, William E. Evans, Mary V. Relling, Wenjian Yang, Jay Shendure, and Douglas M. Fowler. Multiplex assessment of protein variant abundance by massively parallel sequencing. *Nature Genetics*, 50(6):874–882, June 2018. ISSN 1061-4036, 1546-1718. doi: 10.1038/s41588-018-0122-z. URL <https://www.nature.com/articles/s41588-018-0122-z>.

Kenneth A. Matreyek, Jason J. Stephany, Ethan Ahler, and Douglas M. Fowler. Integrating thousands of PTEN variant activity and abundance measurements reveals variant subgroups and new dominant negatives in cancers. *Genome Medicine*, 13(1):165, December 2021. ISSN 1756-994X. doi: 10.1186/s13073-021-00984-x. URL <https://genomemedicine.biomedcentral.com/articles/10.1186/s13073-021-00984-x>.

Florian Mattenberger, Victor Latorre, Omer Tirosh, Adi Stern, and Ron Geller. Globally defining the effects of mutations in a picornavirus capsid. *eLife*, 10:e64256, January 2021. ISSN 2050-084X. doi: 10.7554/eLife.64256. URL <https://elifesciences.org/articles/64256>.

David Mavor, Kyle Barlow, Samuel Thompson, Benjamin A Barad, Alain R Bonny, Clinton L Cario, Garrett Gaskins, Zairan Liu, Laura Deming, Seth D Axen, Elena Caceres, Weilin Chen, Adolfo Cuesta, Rachel E Gate, Evan M Green, Kaitlin R Hulce, Weiyue Ji, Lillian R Kenner, Bruk Mensa, Leanna S Morinishi, Steven M Moss, Marco Mravic, Ryan K Muir, Stefan Niekamp, Chimno I Nnadi, Eugene Palovcak, Erin M Poss, Tyler D Ross, Eugenia C Salcedo, Stephanie K See, Meena Subramaniam, Allison W Wong, Jennifer Li, Kurt S Thorn, Shane Ó Conchúir, Benjamin P Roscoe, Eric D Chow, Joseph L DeRisi, Tanja Kortemme, Daniel N Bolon, and James S Fraser. Determination of ubiquitin fitness landscapes under different chemical stresses in a classroom setting. *eLife*, 5:e15802, April 2016. ISSN 2050-084X. doi: 10.7554/eLife.15802. URL <https://elifesciences.org/articles/15802>.

Richard N. McLaughlin, Jr., Frank J. Poelwijk, Arjun Raman, Walraj S. Gosal, and Rama Ranganathan. The spatial architecture of protein function and adaptation. *Nature*, 491(7422):138–142, November 2012. ISSN 0028-0836, 1476-4687. doi: 10.1038/nature11500. URL <https://www.nature.com/articles/nature11500>.

Gianmarco Meier, Sujani Thavarasah, Kai Ehrenbolger, Cedric A J Hutter, Lea M Hürlimann, Jonas Barandun, and Markus A Seeger. Deep mutational scan of a drug efflux pump reveals its structure-function landscape. *Nature Chemical Biology*, 19(4):440–450, April 2023.

Joshua Meier, Roshan Rao, Robert Verkuil, Jason Liu, Tom Sercu, and Alexander Rives. Language models enable zero-shot prediction of the effects of mutations on protein function. *bioRxiv*, 2021. doi: 10.1101/2021.07.09.450648. URL <https://www.biorxiv.org/content/early/2021/07/10/2021.07.09.450648>.

Iana Meitlis, Eric J. Allenspach, Bradly M. Bauman, Isabelle Q. Phan, Gina Dabbah, Erica G. Schmitt, Nathan D. Camp, Troy R. Torgerson, Deborah A. Nickerson, Michael J. Bamshad, David Hagin, Christopher R. Luthers, Jeffrey R. Stinson, Jessica Gray, Ingrid Lundgren, Joseph A. Church, Manish J. Butte, Mike B. Jordan, Seema S. Aceves, Daniella M. Schwartz, Joshua D. Milner, Susan Schuval, Suzanne Skoda-Smith, Megan A. Cooper, Lea M. Starita, David J. Rawlings, Andrew L. Snow, and Richard G. James. Multiplexed Functional Assessment of Genetic Variants in CARD11. *The American Journal of Human Genetics*, 107(6):1029–1043, December 2020. ISSN 00029297. doi: 10.1016/j.ajhg.2020.10.015. URL <https://linkinghub.elsevier.com/retrieve/pii/S0002929720303736>.

Daniel Melamed, David L. Young, Caitlin E. Gamble, Christina R. Miller, and Stanley Fields. Deep mutational scanning of an RRM domain of the *Saccharomyces cerevisiae* poly(A)-binding protein. *RNA*, 19(11):1537–1551, November 2013. ISSN 1355-8382, 1469-9001. doi: 10.1261/rna.040709.113. URL <http://rnajournal.cshlp.org/lookup/doi/10.1261/rna.040709.113>.

Alexandre Melnikov, Peter Rogov, Li Wang, Andreas Gnarke, and Tarjei S. Mikkelsen. Comprehensive mutational scanning of a kinase *in vivo* reveals substrate-dependent fitness landscapes. *Nucleic Acids Research*, 42(14):e112–e112, August 2014. ISSN 0305-1048, 1362-4962. doi: 10.1093/nar/gku511. URL <https://academic.oup.com/nar/article-lookup/doi/10.1093/nar/gku511>.

Taylor L. Mighell, Sara Evans-Dutson, and Brian J. O’Roak. A Saturation Mutagenesis Approach to Understanding PTEN Lipid Phosphatase Activity and Genotype-Phenotype Relationships. *The American Journal of Human Genetics*, 102(5):943–955, May 2018. ISSN 00029297. doi: 10.1016/j.ajhg.2018.03.018. URL <https://linkinghub.elsevier.com/retrieve/pii/S0002929718301071>.

Peter G. Miller, Murugappan Sathappa, Jamie A. Morocco, Wei Jiang, Yue Qian, Sumaiya Iqbal, Qi Guo, Andrew O. Giacomelli, Subrata Shaw, Camille Vernier, Besnik Bajrami, Xiaoping Yang, Cerise Raffier, Adam S. Sperling, Christopher J. Gibson, Josephine Kahn, Cyrus Jin, Matthew Ranaghan, Alisha Caliman, Merissa Brousseau, Eric S. Fischer, Robert Lintner, Federica Piccioni, Arthur J. Campbell, David E. Root, Colin W. Garvie, and Benjamin L. Ebert. Allosteric inhibition of PPM1D serine/threonine phosphatase via an altered conformational state. *Nature Communications*, 13(1):3778, June 2022. ISSN 2041-1723. doi: 10.1038/s41467-022-30463-9. URL <https://www.nature.com/articles/s41467-022-30463-9>.

Parul Mishra, Julia M. Flynn, Tyler N. Starr, and Daniel N.A. Bolon. Systematic Mutant Analyses Elucidate General and Client-Specific Aspects of Hsp90 Function. *Cell Reports*, 15(3):588–598, April 2016. ISSN 22111247. doi: 10.1016/j.celrep.2016.03.046. URL <https://linkinghub.elsevier.com/retrieve/pii/S2211124716303175>.

Iain H. Moal and Juan Fernández-Recio. SKEMPI: a structural kinetic and energetic database of mutant protein interactions and its use in empirical models. *Bioinformatics*, 28 20:2600–7, 2012.

Ayesha Muhammad, Maria E Calandranis, Bian Li, Tao Yang, Daniel J Blackwell, M Lorena Harvey, Jeremy E Smith, Ashli E Chew, John A Capra, Kenneth A Matreyek, Douglas M Fowler, Dan M Roden, and Andrew M Glazer. High-throughput functional mapping of variants in an arrhythmia gene, KCNE1, reveals novel biology. *bioRxiv*, April 2023.

Robert W. Newberry, Taylor Arhar, Jean Costello, George C. Hartoularios, Alison M. Maxwell, Zun Zar Chi Naing, Maureen Pittman, Nishith R. Reddy, Daniel M. C. Schwarz, Douglas R. Wassarman, Taia S. Wu, Daniel Barrero, Christa Caggiano, Adam Catching, Taylor B. Cavazos, Laurel S. Estes, Bryan Faust, Elissa A. Fink, Miriam A. Goldman, Yessica K. Gomez, M. Grace Gordon, Laura M. Gunsalus, Nick Hoppe, Maru Jaime-Garza, Matthew C. Johnson, Matthew G. Jones, Andrew F. Kung, Kyle E. Lopez, Jared Lumpe, Calla Martyn, Elizabeth E. McCarthy, Lakshmi E. Miller-Vedam, Erik J. Navarro, Aji Palar, Jenna Pellegrino, Wren Saylor, Christina A. Stephens, Jack Strickland, Hayarpi Torosyan, Stephanie A. Wankowicz, Daniel R. Wong, Garrett Wong, Sy Redding, Eric D. Chow, William F. DeGrado, and Martin Kampmann. Robust Sequence Determinants of alpha-Synuclein Toxicity in Yeast Implicate Membrane Binding. *ACS Chemical Biology*, 15(8):2137–2153, August 2020. ISSN 1554-8929, 1554-8937. doi: 10.1021/acschembio.0c00339. URL <https://pubs.acs.org/doi/10.1021/acschembio.0c00339>.

Pauline C Ng and Steven Henikoff. Accounting for human polymorphisms predicted to affect protein function. *Genome Res.*, 12(3):436–446, March 2002.

Thuy N Nguyen, Christine Ingle, Samuel Thompson, and Kimberly A Reynolds. The genetic landscape of a metabolic interaction. May 2023a.

Vanessa Nguyen, Ethan Ahler, Katherine A Sitko, Jason J Stephany, Dustin J Maly, and Douglas M Fowler. Molecular determinants of hsp90 dependence of src kinase revealed by deep mutational scanning. *Protein Science*, 32(7):e4656, July 2023b.

Erik Nijkamp, Jeffrey A. Ruffolo, Eli N. Weinstein, Nikhil Naik, and Ali Madani. ProGen2: Exploring the boundaries of protein language models. *ArXiv*, abs/2206.13517, 2022.

Pascal Notin, Mafalda Dias, Jonathan Frazer, Javier Marchena-Hurtado, Aidan N. Gomez, Debora S. Marks, and Yarin Gal. Tranception: protein fitness prediction with autoregressive transformers and inference-time retrieval. In *ICML*, 2022a.

Pascal Notin, Lood Van Niekerk, Aaron W. Kollasch, Daniel Ritter, Yarin Gal, and Debora Susan Marks. TranceptEVE: Combining Family-specific and Family-agnostic Models of Protein Sequences for Improved Fitness Prediction. December 2022b. URL <https://openreview.net/forum?id=170o9DcLmR1>.

Pascal Notin, Ruben Weitzman, Debora S. Marks, and Yarin Gal. ProteinNPT: Improving protein property prediction and design with non-parametric transformers. *Advances in Neural Information Processing Systems*, 37, 2023.

Christina Nutschel, Alexander Fulton, Olav Zimmermann, Ulrich Schwaneberg, Karl-Erich Jaeger, and Holger Gohlke. Systematically Scrutinizing the Impact of Substitution Sites on Thermostability and Detergent Tolerance for *Bacillus subtilis* Lipase A. *Journal of Chemical Information and Modeling*, 60(3):1568–1584, March 2020. ISSN 1549-9596, 1549-960X. doi: 10.1021/acs.jcim.9b00954. URL <https://pubs.acs.org/doi/10.1021/acs.jcim.9b00954>.

C. Anders Olson, Nicholas C. Wu, and Ren Sun. A Comprehensive Biophysical Description of Pairwise Epistasis throughout an Entire Protein Domain. *Current Biology*, 24(22):2643–2651, November 2014. ISSN 09609822. doi: 10.1016/j.cub.2014.09.072. URL <https://linkinghub.elsevier.com/retrieve/pii/S0960982214012688>.

Martin K Ostermaier, Christian Peterhans, Rolf Jaussi, Xavier Deupi, and Jörg Standfuss. Functional map of arrestin-1 at single amino acid resolution. *Proceedings of the National Academy of Sciences*, 111(5):1825–1830, February 2014.

Vikas Pejaver, Alicia B Byrne, Bing-Jian Feng, Kymberleigh A Pagel, Sean D Mooney, Rachel Karchin, Anne O'Donnell-Luria, Steven M Harrison, Sean V Tavtigian, Marc S Greenblatt, et al. Calibration of computational tools for missense variant pathogenicity classification and clingen recommendations for pp3/bp4 criteria. *The American Journal of Human Genetics*, 109(12):2163–2177, 2022.

Victoria O. Pokusaeva, Dinara R. Usmanova, Ekaterina V. Putintseva, Lorena Espinar, Karen S. Sarkisyan, Alexander S. Mishin, Natalya S. Bogatyreva, Dmitry N. Ivankov, Arseniy V. Akopyan, Sergey Ya. Avvakumov, Inna S. Povolotskaya, Guillaume J. Filion, Lucas B. Carey, and Fyodor A. Kondrashov. An experimental assay of the interactions of amino acids from orthologous sequences shaping a complex fitness landscape. *PLOS Genetics*, 15(4):e1008079, April 2019. ISSN 1553-7404. doi: 10.1371/journal.pgen.1008079. URL <https://dx.plos.org/10.1371/journal.pgen.1008079>.

Hangfei Qi, C. Anders Olson, Nicholas C. Wu, Ruiyan Ke, Claude Loverdo, Virginia Chu, Shawna Truong, Roland Remenyi, Zugen Chen, Yushen Du, Sheng-Yao Su, Laith Q. Al-Mawsawi, Ting-Ting Wu, Shu-Hua Chen, Chung-Yen Lin, Weidong Zhong, James O. Lloyd-Smith, and Ren Sun. A Quantitative High-Resolution Genetic Profile Rapidly Identifies Sequence Determinants of Hepatitis C Viral Fitness and Drug Sensitivity. *PLoS Pathogens*, 10(4):e1004064, April 2014. ISSN 1553-7374. doi: 10.1371/journal.ppat.1004064. URL <https://dx.plos.org/10.1371/journal.ppat.1004064>.

Daniel Quang, Yifei Chen, and Xiaohui Xie. DANN: a deep learning approach for annotating the pathogenicity of genetic variants. *Bioinformatics*, 31(5):761–763, 2015.

Alec Radford, Jeff Wu, Rewon Child, David Luan, Dario Amodei, and Ilya Sutskever. Language models are unsupervised multitask learners. 2019. URL <https://api.semanticscholar.org/CorpusID:160025533>.

Daniele Raimondi, Ibrahim Tanyalcin, Julien Ferté, Andrea Gazzo, Gabriele Orlando, Tom Lenaerts, Marianne Rooman, and Wim Vranken. DEOGEN2: prediction and interactive visualization of single amino acid variant deleteriousness in human proteins. *Nucleic acids research*, 45(W1):W201–W206, 2017.

Roshan Rao, Nicholas Bhattacharya, Neil Thomas, Yan Duan, Xi Chen, John Canny, Pieter Abbeel, and Yun S. Song. Evaluating Protein Transfer Learning with TAPE, June 2019. URL <http://arxiv.org/abs/1906.08230> [cs, q-bio, stat].

Roshan Rao, Jason Liu, Robert Verkuil, Joshua Meier, John F. Canny, Pieter Abbeel, Tom Sercu, and Alexander Rives. MSA transformer. *bioRxiv*, 2021. doi: 10.1101/2021.02.12.430858. URL <https://www.biorxiv.org/content/early/2021/02/13/2021.02.12.430858>.

Philipp Rentzsch, Daniela Witten, Gregory M Cooper, Jay Shendure, and Martin Kircher. Cadd: predicting the deleteriousness of variants throughout the human genome. *Nucleic acids research*, 47(D1):D886–D894, 2019.

Boris Reva, Yevgeniy Antipin, and Chris Sander. Predicting the functional impact of protein mutations: application to cancer genomics. *Nucleic Acids Research*, 39(17):e118, September 2011. ISSN 1362-4962. doi: 10.1093/nar/gkr407.

Adam J Riesselman, John B Ingraham, and Debora S Marks. Deep generative models of genetic variation capture the effects of mutations. *Nature Methods*, 15(10):816–822, 2018.

Alexander Rives, Joshua Meier, Tom Sercu, Siddharth Goyal, Zeming Lin, Jason Liu, Demi Guo, Myle Ott, C Lawrence Zitnick, Jerry Ma, et al. Biological structure and function emerge from scaling unsupervised learning to 250 million protein sequences. *Proceedings of the National Academy of Sciences*, 118(15), 2021.

Liat Rockah-Shmuel, Ágnes Tóth-Petróczy, and Dan S. Tawfik. Systematic Mapping of Protein Mutational Space by Prolonged Drift Reveals the Deleterious Effects of Seemingly Neutral Mutations. *PLOS Computational Biology*, 11(8):e1004421, August 2015. ISSN 1553-7358. doi: 10.1371/journal.pcbi.1004421. URL <https://dx.plos.org/10.1371/journal.pcbi.1004421>.

Philip A. Romero, Andreas Krause, and Frances H. Arnold. Navigating the protein fitness landscape with gaussian processes. *Proceedings of the National Academy of Sciences*, 110:E193 – E201, 2012. URL <https://api.semanticscholar.org/CorpusID:1093192>.

Philip A. Romero, Tuan M. Tran, and Adam R. Abate. Dissecting enzyme function with microfluidic-based deep mutational scanning. *Proceedings of the National Academy of Sciences*, 112(23):7159–7164, June 2015. ISSN 0027-8424, 1091-6490. doi: 10.1073/pnas.1422285112. URL <https://pnas.org/doi/full/10.1073/pnas.1422285112>.

Benjamin P. Roscoe and Daniel N.A. Bolon. Systematic Exploration of Ubiquitin Sequence, E1 Activation Efficiency, and Experimental Fitness in Yeast. *Journal of Molecular Biology*, 426(15):2854–2870, July 2014. ISSN 00222836. doi: 10.1016/j.jmb.2014.05.019. URL <https://linkinghub.elsevier.com/retrieve/pii/S0022283614002587>.

Benjamin P. Roscoe, Kelly M. Thayer, Konstantin B. Zeldovich, David Fushman, and Daniel N.A. Bolon. Analyses of the Effects of All Ubiquitin Point Mutants on Yeast Growth Rate. *Journal of Molecular Biology*, 425(8):1363–1377, April 2013. ISSN 00222836. doi: 10.1016/j.jmb.2013.01.032. URL <https://linkinghub.elsevier.com/retrieve/pii/S0022283613000636>.

Hridindu Roychowdhury and Philip A Romero. Microfluidic deep mutational scanning of the human executioner caspases reveals differences in structure and regulation. *Cell Death Discovery*, 8(1):7, January 2022.

Alan F. Rubin, Joseph K Min, Nathan J. Rollins, Estelle Y Da, Daniel Esposito, Matthew Harrington, Jeremy Stone, Aisha Haley Bianchi, Mafalda Dias, Jonathan Frazer, Yunfan Fu, Molly Gallaher, Iris Li, Olivia Moscatelli, Jesslyn YL Ong, Joshua E Rollins, Matthew J. Wakefield, Shenyi “Sunny” Ye, Amy Sze Pui Tam, Abbye E. McEwen, Lea M. Starita, Vanessa L. Bryant, Debora S. Marks, and Douglas M. Fowler. MaveDB v2: a curated community database with over three million variant effects from multiplexed functional assays. *bioRxiv*, 2021.

William P. Russ, Matteo Figliuzzi, Christian Stocker, Pierre Barrat-Charlaix, Michael Socolich, Peter Kast, Donald Hilvert, Remi Monasson, Simona Cocco, Martin Weigt, and Rama Ranganathan. An evolution-based model for designing chorismate mutase enzymes. *Science*, 369(6502):440–445, July 2020. ISSN 0036-8075, 1095-9203. doi: 10.1126/science.aba3304. URL <https://www.science.org/lookup/doi/10.1126/science.aba3304>.

Kaitlin E Samocha, Jack A Kosmicki, Konrad J Karczewski, Anne H O’Donnell-Luria, Emma Pierce-Hoffman, Daniel G MacArthur, Benjamin M Neale, and Mark J Daly. Regional missense constraint improves variant deleteriousness prediction. *BioRxiv*, page 148353, 2017.

Karen S. Sarkisyan, Dmitry A. Bolotin, Margarita V. Meer, Dinara R. Usmanova, Alexander S. Mishin, George V. Sharonov, Dmitry N. Ivankov, Nina G. Bozhanova, Mikhail S. Baranov, Onuralp Soylemez, Natalya S. Bogatyreva, Peter K. Vlasov, Evgeny S. Egorov, Maria D. Logacheva, Alexey S. Kondrashov, Dmitry M. Chudakov, Ekaterina V. Putintseva, Ilgar Z. Mamedov, Dan S. Tawfik, Konstantin A. Lukyanov, and Fyodor A. Kondrashov. Local fitness landscape of the green fluorescent protein. *Nature*, 533(7603):397–401, May 2016. ISSN 0028-0836, 1476-4687. doi: 10.1038/nature17995. URL <http://www.nature.com/articles/nature17995>.

Jana Marie Schwarz, Christian Rödelsperger, Markus Schuelke, and Dominik Seelow. MutationTaster evaluates disease-causing potential of sequence alterations. *Nature methods*, 7(8):575–576, 2010.

Mireia Seuma, Andre J Faure, Marta Badia, Ben Lehner, and Benedetta Bolognesi. The genetic landscape for amyloid beta fibril nucleation accurately discriminates familial Alzheimer’s disease mutations. *eLife*, 10: e63364, February 2021. ISSN 2050-084X. doi: 10.7554/eLife.63364. URL <https://elifesciences.org/articles/63364>.

Mireia Seuma, Ben Lehner, and Benedetta Bolognesi. An atlas of amyloid aggregation: the impact of substitutions, insertions, deletions and truncations on amyloid beta fibril nucleation. *Nature Communications*, 13(1): 7084, November 2022.

Hashem A Shihab, Julian Gough, David N Cooper, Peter D Stenson, Gary LA Barker, Keith J Edwards, Ian NM Day, and Tom R Gaunt. Predicting the functional, molecular, and phenotypic consequences of amino acid substitutions using hidden markov models. *Human mutation*, 34(1):57–65, 2013.

Jung-Eun Shin, Adam J Riesselman, Aaron W Kollasch, Conor McMahon, Elana Simon, Chris Sander, Aashish Manglik, Andrew C Kruse, and Debora S Marks. Protein design and variant prediction using autoregressive generative models. *Nature communications*, 12(1):1–11, 2021.

D Shortle and J Sondek. The emerging role of insertions and deletions in protein engineering. *Curr. Opin. Biotechnol.*, 6(4):387–393, August 1995.

Rachel A. Silverstein, Song Sun, Marta Verby, Jochen Weile, Yingzhou Wu, Marinella Gebbia, Iosifina Fotiadou, Julia Kitaygorodsky, and Frederick P. Roth. A systematic genotype-phenotype map for missense variants in the human intellectual disability-associated gene *GDII*. preprint, Genetics, October 2021. URL <http://biorxiv.org/lookup/doi/10.1101/2021.10.06.463360>.

Sam Sinai, Nina Jain, George M Church, and Eric D Kelsic. Generative AAV capsid diversification by latent interpolation. preprint, Synthetic Biology, April 2021. URL <http://biorxiv.org/lookup/doi/10.1101/2021.04.16.440236>.

Yq Shirleen Soh, Louise H Moncla, Rachel Eguia, Trevor Bedford, and Jesse D Bloom. Comprehensive mapping of adaptation of the avian influenza polymerase protein PB2 to humans. *eLife*, 8:e45079, April 2019. ISSN 2050-084X. doi: 10.7554/eLife.45079. URL <https://elifesciences.org/articles/45079>.

Marion Sourisseau, Daniel J. P. Lawrence, Megan C. Schwarz, Carina H. Storrs, Ethan C. Veit, Jesse D. Bloom, and Matthew J. Evans. Deep Mutational Scanning Comprehensively Maps How Zika Envelope Protein Mutations Affect Viral Growth and Antibody Escape. *Journal of Virology*, 93(23):e01291–19, December 2019. ISSN 0022-538X, 1098-5514. doi: 10.1128/JVI.01291-19. URL <https://journals.asm.org/doi/10.1128/JVI.01291-19>.

Jeffrey M. Spencer and Xiaoliu Zhang. Deep mutational scanning of *S. pyogenes* Cas9 reveals important functional domains. *Scientific Reports*, 7(1):16836, December 2017. ISSN 2045-2322. doi: 10.1038/s41598-017-17081-y. URL <https://www.nature.com/articles/s41598-017-17081-y>.

Tobias Stadelmann, Daniel Heid, Michael Jendrusch, Jan Mathony, Stéphane Rosset, Bruno E. Correia, and Dominik Niopek. A deep mutational scanning platform to characterize the fitness landscape of anti-CRISPR proteins. preprint, Synthetic Biology, August 2021. URL <http://biorxiv.org/lookup/doi/10.1101/2021.08.21.457204>.

Max V. Staller, Alex S. Holehouse, Devjanee Swain-Lenz, Rahul K. Das, Rohit V. Pappu, and Barak A. Cohen. A High-Throughput Mutational Scan of an Intrinsically Disordered Acidic Transcriptional Activation Domain. *Cell Systems*, 6(4):444–455.e6, April 2018. ISSN 24054712. doi: 10.1016/j.cels.2018.01.015. URL <https://linkinghub.elsevier.com/retrieve/pii/S2405471218300528>.

Lea M. Starita, Jonathan N. Pruneda, Russell S. Lo, Douglas M. Fowler, Helen J. Kim, Joseph B. Hiatt, Jay Shendure, Peter S. Brzovic, Stanley Fields, and Rachel E. Klevit. Activity-enhancing mutations in an E3 ubiquitin ligase identified by high-throughput mutagenesis. *Proceedings of the National Academy of Sciences*, 110(14), April 2013. ISSN 0027-8424, 1091-6490. doi: 10.1073/pnas.1303309110. URL <https://pnas.org/doi/full/10.1073/pnas.1303309110>.

Tyler N. Starr, Allison J. Greaney, Sarah K. Hilton, Daniel Ellis, Katharine H.D. Crawford, Adam S. Dingens, Mary Jane Navarro, John E. Bowen, M. Alejandra Tortorici, Alexandra C. Walls, Neil P. King, David Veesler, and Jesse D. Bloom. Deep Mutational Scanning of SARS-CoV-2 Receptor Binding Domain Reveals Constraints on Folding and ACE2 Binding. *Cell*, 182(5):1295–1310.e20, September 2020. ISSN 00928674. doi: 10.1016/j.cell.2020.08.012. URL <https://linkinghub.elsevier.com/retrieve/pii/S0092867420310035>.

Martin Steinegger and Johannes Söding. Clustering huge protein sequence sets in linear time. *Nature Communications*, 9(1):2542, Jun 2018. ISSN 2041-1723. doi: 10.1038/s41467-018-04964-5. URL <https://doi.org/10.1038/s41467-018-04964-5>.

Michael A. Stiffler, Doeke R. Hekstra, and Rama Ranganathan. Evolvability as a Function of Purifying Selection in TEM-1 beta-Lactamase. *Cell*, 160(5):882–892, February 2015. ISSN 00928674. doi: 10.1016/j.cell.2015.01.035. URL <https://linkinghub.elsevier.com/retrieve/pii/S0092867415000781>.

Jan Stourac, Juraj Dúbrava, Miloš Musil, Jana Horáčková, Jiří Damborský, S. Mazurenko, and David Bednář. FireProtDB: database of manually curated protein stability data. *Nucleic Acids Research*, 49:D319 – D324, 2020.

Chase C. Suiter, Takaya Moriyama, Kenneth A. Matreyek, Wentao Yang, Emma Rose Scaletti, Rina Nishii, Wenzian Yang, Keito Hoshitsuki, Minu Singh, Amita Trehan, Chris Parish, Colton Smith, Lie Li, Deepa Bhojwani, Liz Y. P. Yuen, Chi-kong Li, Chak-ho Li, Yung-li Yang, Gareth J. Walker, James R. Goodhand, Nicholas A. Kennedy, Federico Antillon Klussmann, Smita Bhatia, Mary V. Relling, Motohiro Kato, Hiroki Hori, Prateek Bhatia, Tariq Ahmad, Allen E. J. Yeoh, Pál Stenmark, Douglas M. Fowler, and Jun J. Yang. Massively parallel variant characterization identifies *NUDT15* alleles associated with thiopurine toxicity. *Proceedings of the National Academy of Sciences*, 117(10):5394–5401, March 2020. ISSN 0027-8424, 1091-6490. doi: 10.1073/pnas.1915680117. URL <https://pnas.org/doi/full/10.1073/pnas.1915680117>.

Song Sun, Jochen Weile, Marta Verby, Yingzhou Wu, Yang Wang, Atina G. Cote, Iosifina Fotiadou, Julia Kitaygorodsky, Marc Vidal, Jasper Rine, Pavel Ješina, Viktor Kožich, and Frederick P. Roth. A proactive genotype-to-patient-phenotype map for cystathionine beta-synthase. *Genome Medicine*, 12(1):13, December 2020. ISSN 1756-994X. doi: 10.1186/s13073-020-0711-1. URL <https://genomemedicine.biomedcentral.com/articles/10.1186/s13073-020-0711-1>.

Laksshman Sundaram, Hong Gao, Samskruthi Reddy Padigepati, Jeremy F McRae, Yanjun Li, Jack A Kosmicki, Nondas Fritzilas, Jörg Hakenberg, Anindita Dutta, John Shon, et al. Predicting the clinical impact of human mutation with deep neural networks. *Nature genetics*, 50(8):1161–1170, 2018.

Amporn Suphatrakul, Pratsaneeyaporn Posiri, Nittaya Srisuk, Rapirat Nantachokchawapan, Suppachoke Onome, Juthathip Mongkolsapaya, and Bumpote Siridechadilok. Functional analysis of flavivirus replicase by deep mutational scanning of dengue NS5. March 2023.

Baris E. Suzek, Yuqi Wang, Hongzhan Huang, Peter B. McGarvey, and Cathy H. Wu. UniRef clusters: a comprehensive and scalable alternative for improving sequence similarity searches. *Bioinformatics*, 31:926 – 932, 2014.

Baris E Suzek, Yuqi Wang, Hongzhan Huang, Peter B McGarvey, Cathy H Wu, and UniProt Consortium. UniRef clusters: a comprehensive and scalable alternative for improving sequence similarity searches. *Bioinformatics*, 31(6):926–932, 2015.

Timothy J C Tan, Zongjun Mou, Ruipeng Lei, Wenhao O Ouyang, Meng Yuan, Ge Song, Raiees Andrabi, Ian A Wilson, Collin Kieffer, Xinghong Dai, Kenneth A Matreyek, and Nicholas C Wu. High-throughput identification of prefusion-stabilizing mutations in SARS-CoV-2 spike. *Nature Communications*, 14(1):2003, April 2023.

Samuel Thompson, Yang Zhang, Christine Ingle, Kimberly A Reynolds, and Tanja Kortemme. Altered expression of a quality control protease in *E. coli* reshapes the *in vivo* mutational landscape of a model enzyme. *eLife*, 9: e53476, July 2020. ISSN 2050-084X. doi: 10.7554/eLife.53476. URL <https://elifesciences.org/articles/53476>.

Bargavi Thyagarajan and Jesse D Bloom. The inherent mutational tolerance and antigenic evolvability of influenza hemagglutinin. *Elife*, 3, July 2014.

Agnes Tóth-Petróczy and Dan S Tawfik. Protein insertions and deletions enabled by neutral roaming in sequence space. *Mol. Biol. Evol.*, 30(4):761–771, April 2013.

Arti Tripathi, Kritika Gupta, Shruti Khare, Pankaj C. Jain, Siddharth Patel, Prasanth Kumar, Ajai J. Pulianmackal, Nilesh Aghera, and Raghavan Varadarajan. Molecular Determinants of Mutant Phenotypes, Inferred from Saturation Mutagenesis Data. *Molecular Biology and Evolution*, 33(11):2960–2975, November 2016. ISSN 0737-4038, 1537-1719. doi: 10.1093/molbev/msw182. URL <https://academic.oup.com/mbe/article-lookup/doi/10.1093/molbev/msw182>.

Kotaro Tsuboyama, Justas Dauparas, Jonathan Chen, Elodie Laine, Yasser Mohseni Behbahani, Jonathan J. Weinstein, Niall M. Mangan, Sergey Ovchinnikov, and Gabriel J. Rocklin. Mega-scale experimental analysis of protein folding stability in biology and protein design, December 2022. URL <https://www.biorxiv.org/content/10.1101/2022.12.06.519132v3>. Pages: 2022.12.06.519132 Section: New Results.

Kotaro Tsuboyama, Justas Dauparas, Jonathan Chen, Elodie Laine, Yasser Mohseni Behbahani, Jonathan J. Weinstein, Niall M. Mangan, Sergey Ovchinnikov, and Gabriel J. Rocklin. Mega-scale experimental analysis of protein folding stability in biology and design. *Nature*, 620(7973):434–444, August 2023. ISSN 0028-0836, 1476-4687. doi: 10.1038/s41586-023-06328-6. URL <https://www.nature.com/articles/s41586-023-06328-6>.

UK Monogenic Diabetes Consortium, Myocardial Infarction Genetics Consortium, UK Congenital Lipodystrophy Consortium, Amit R Majithia, Ben Tsuda, Maura Agostini, Keerthana Gnanapradeepan, Robert Rice, Gina Peloso, Kashyap A Patel, Xiaolan Zhang, Marjoleine F Broekema, Nick Patterson, Marc Duby, Ted Sharpe, Eric Kalkhoven, Evan D Rosen, Inês Barroso, Sian Ellard, Sekar Kathiresan, Stephen O’Rahilly, Krishna Chatterjee, Jose C Florez, Tarjei Mikkelsen, David B Savage, and David Altshuler. Prospective functional classification of all possible missense variants in PPARG. *Nature Genetics*, 48(12):1570–1575, December 2016. ISSN 1061-4036, 1546-1718. doi: 10.1038/ng.3700. URL <https://www.nature.com/articles/ng.3700>.

Fabio Urbina, Filippa Lentzos, Cédric Invernizzi, and Sean Ekins. Dual use of artificial-intelligence-powered drug discovery. *Nature Machine Intelligence*, 4(3):189–191, 2022.

Oana Ursu, James T Neal, Emily Shea, Pratiksha I Thakore, Livnat Jerby-Arnon, Lan Nguyen, Danielle Dionne, Celeste Diaz, Julia Bauman, Mariam Mounir Mosaad, Christian Fagre, April Lo, Maria McSharry, Andrew O Giacomelli, Seav Huong Ly, Orit Rozenblatt-Rosen, William C Hahn, Andrew J Aguirre, Alice H Berger, Aviv Regev, and Jesse S Boehm. Massively parallel phenotyping of coding variants in cancer with perturb-seq. *Nature Biotechnology*, 40(6):896–905, June 2022.

Warren van Loggerenberg, Shahin Sowlati-Hashjin, Jochen Weile, Rayna Hamilton, Aditya Chawla, Marinella Gebbia, Nishka Kishore, Laure Frésard, Sami Mustajoki, Elena Pischik, Elena Di Pierro, Michela Barbaro, Ylva Floderus, Caroline Schmitt, Laurent Gouya, Alexandre Colavin, Robert Nussbaum, Edith C H Friesema, Raili Kauppinen, Jordi To-Figueras, Aasne K Aarsand, Robert J Desnick, Michael Garton, and Frederick P Roth. Systematically testing human HMBS missense variants to reveal mechanism and pathogenic variation. *bioRxiv*, February 2023.

Rosario Vanella, Christoph Küng, Alexandre A Schoepfer, Vanni Doffini, Jin Ren, and Michael A Nash. Understanding Activity-Stability tradeoffs in biocatalysts by enzyme proximity sequencing. March 2023.

Ashish Vaswani, Noam Shazeer, Niki Parmar, Jakob Uszkoreit, Llion Jones, Aidan N. Gomez, Lukasz Kaiser, and Illia Polosukhin. Attention is all you need, 2017.

Veeramohan Veerapandian, Jan Ole Ackermann, Yogesh Srivastava, Vikas Malik, Mingxi Weng, Xiaoxiao Yang, and Ralf Jauch. Directed evolution of reprogramming factors by cell selection and sequencing. *Stem Cell Reports*, 11(2):593–606, August 2018.

Aliete Wan, Emily Place, Eric A. Pierce, and Jason Comander. Characterizing variants of unknown significance in rhodopsin: A functional genomics approach. *Human Mutation*, 40(8):1127–1144, August 2019. ISSN 1059-7794, 1098-1004. doi: 10.1002/humu.23762. URL <https://onlinelibrary.wiley.com/doi/10.1002/humu.23762>.

Ryan Weeks and Marc Ostermeier. Fitness and functional landscapes of the *e. coli* RNase III gene *rnc*. *Molecular Biology and Evolution*, 40(3), March 2023.

Jochen Weile, Song Sun, Atina G Cote, Jennifer Knapp, Marta Verby, Joseph C Mellor, Yingzhou Wu, Carles Pons, Cassandra Wong, Natascha Lieshout, Fan Yang, Murat Tasan, Guihong Tan, Shan Yang, Douglas M Fowler, Robert Nussbaum, Jesse D Bloom, Marc Vidal, David E Hill, Patrick Aloy, and Frederick P Roth. A framework for exhaustively mapping functional missense variants. *Molecular Systems Biology*, 13(12):957, December 2017. ISSN 1744-4292, 1744-4292. doi: 10.15252/msb.20177908. URL <https://onlinelibrary.wiley.com/doi/10.15252/msb.20177908>.

Jochen Weile, Nishka Kishore, Song Sun, Ranim Maaieh, Marta Verby, Roujia Li, Iosifina Fotiadou, Julia Kitaygorodsky, Yingzhou Wu, Alexander Holenstein, Céline Bürer, Linnea Blomgren, Shan Yang, Robert Nussbaum, Rima Rozen, David Watkins, Marinella Gebbia, Viktor Kozich, Michael Garton, D Sean Froese, and Frederick P Roth. Shifting landscapes of human MTHFR missense-variant effects. *American Journal of Human Genetics*, 108(7):1283–1300, July 2021.

Chenchun Weng, Andre J Faure, and Ben Lehner. The energetic and allosteric landscape for KRAS inhibition. December 2022.

Emily E. Wrenbeck, Laura R. Azouz, and Timothy A. Whitehead. Single-mutation fitness landscapes for an enzyme on multiple substrates reveal specificity is globally encoded. *Nature Communications*, 8(1):15695, August 2017. ISSN 2041-1723. doi: 10.1038/ncomms15695. URL <http://www.nature.com/articles/ncomms15695>.

Emily E Wrenbeck, Matthew A Bedewitz, Justin R Klesmith, Syeda Noshin, Cornelius S Barry, and Timothy A Whitehead. An automated Data-Driven pipeline for improving heterologous enzyme expression. *ACS Synthetic Biology*, 8(3):474–481, March 2019.

Nicholas C. Wu, Arthur P. Young, Laith Q. Al-Mawsawi, C. Anders Olson, Jun Feng, Hangfei Qi, Shu-Hwa Chen, I.-Hsuan Lu, Chung-Yen Lin, Robert G. Chin, Harding H. Luan, Nguyen Nguyen, Stanley F. Nelson, Xinmin Li, Ting-Ting Wu, and Ren Sun. High-throughput profiling of influenza A virus hemagglutinin gene at single-nucleotide resolution. *Scientific Reports*, 4(1):4942, December 2014. ISSN 2045-2322. doi: 10.1038/srep04942. URL <https://www.nature.com/articles/srep04942>.

Nicholas C. Wu, C. Anders Olson, Yushen Du, Shuai Le, Kevin Tran, Roland Remenyi, Danyang Gong, Laith Q. Al-Mawsawi, Hangfei Qi, Ting-Ting Wu, and Ren Sun. Functional Constraint Profiling of a Viral Protein Reveals Discordance of Evolutionary Conservation and Functionality. *PLOS Genetics*, 11(7):e1005310, July 2015. ISSN 1553-7404. doi: 10.1371/journal.pgen.1005310. URL <https://dx.plos.org/10.1371/journal.pgen.1005310>.

Nicholas C Wu, Lei Dai, C Anders Olson, James O Lloyd-Smith, and Ren Sun. Adaptation in protein fitness landscapes is facilitated by indirect paths. *eLife*, 5:e16965, July 2016. ISSN 2050-084X. doi: 10.7554/eLife.16965. URL <https://elifesciences.org/articles/16965>.

Yingzhou Wu, Hanqing Liu, Roujia Li, Song Sun, Jochen Weile, and Frederick P Roth. Improved pathogenicity prediction for rare human missense variants. *The American Journal of Human Genetics*, 108(10):1891–1906, 2021.

Zachary Wu, S. B. Jennifer Kan, Russell D. Lewis, Bruce J. Wittmann, and Frances H. Arnold. Machine learning-assisted directed protein evolution with combinatorial libraries. *Proceedings of the National Academy of Sciences*, 116:8852 – 8858, 2019. URL <https://api.semanticscholar.org/CorpusID:67770057>.

Michael J Xie, Gareth A Cromie, Katherine Owens, Martin S Timour, Michelle Tang, J Nathan Kutz, Ayman W El-Hattab, Richard N McLaughlin, and Aimée M Dudley. Predicting the functional effect of compound heterozygous genotypes from large scale variant effect maps. *bioRxiv*, January 2023.

Minghao Xu, Zuobai Zhang, Jiarui Lu, Zhaocheng Zhu, Yangtian Zhang, Chang Ma, Runcheng Liu, and Jian Tang. PEER: A Comprehensive and Multi-Task Benchmark for Protein Sequence Understanding, September 2022. URL <http://arxiv.org/abs/2206.02096>. arXiv:2206.02096 [cs].

Kevin Kaichuang Yang, Zachary Wu, and Frances H. Arnold. Machine-learning-guided directed evolution for protein engineering. *Nature Methods*, pages 1–8, 2018. URL <https://api.semanticscholar.org/CorpusID:128342395>.

Kevin Kaichuang Yang, Alex X. Lu, and Nicoló Fusi. Convolutions are competitive with transformers for protein sequence pretraining. *bioRxiv*, 2023a. URL <https://api.semanticscholar.org/CorpusID:248990392>.

Kevin Kaichuang Yang, Niccoló Zanichelli, and Hugh Yeh. Masked inverse folding with sequence transfer for protein representation learning. *bioRxiv*, 2023b. URL <https://api.semanticscholar.org/CorpusID:249241961>.

Sook Wah Yee, Christian Macdonald, Darko Mitrovic, Xujia Zhou, Megan L Koleske, Jia Yang, Dina Buitrago Silva, Patrick Rockefeller Grimes, Donovan Trinidad, Swati S More, Linda Kachuri, John S Witte, Lucie Delemotte, Kathleen M Giacomini, and Willow Coyote-Maestas. The full spectrum of OCT1 (SLC22A1) mutations bridges transporter biophysics to drug pharmacogenomics. *bioRxiv*, June 2023.

Heather J. Young, Matthew Chan, Balaji Selvam, Steven K. Szymanski, Diwakar Shukla, and Erik Procko. Deep Mutagenesis of a Transporter for Uptake of a Non-Native Substrate Identifies Conformationally Dynamic Regions. preprint, Biochemistry, April 2021. URL <http://biorxiv.org/lookup/doi/10.1101/2021.04.19.440442>.

Haicang Zhang, Michelle S Xu, Xiao Fan, Wendy K Chung, and Yufeng Shen. Predicting functional effect of missense variants using graph attention neural networks. *Nature Machine Intelligence*, 4(11):1017–1028, 2022.

Naihui Zhou, Yuxiang Jiang, Timothy Bergquist, Alexandra J. Lee, Balint Z. Kacsoh, Alex Crocker, Kimberley A. Lewis, George E. Georgiou, Huy N. Nguyen, Nafiz Imtiaz Bin Hamid, Larry Davis, Tunca Dogan, Volkan Atalay, Ahmet Sureyya Rifaioglu, Alperen Dalkiran, Rengul Cetin-Atalay, Chengxin Zhang, Rebecca L. Hurto, Peter L. Freddolino, Yang Zhang, Prajwal Bhat, Fran Supek, José María Fernández, Branislava Gemović, Vladimir Perovic, Radoslav Davidovic, Nevena Veljkovic, Ehsaneddin Asgari, Mohammad R. K. Mofrad, Giuseppe Profiti, Castrense Savoardo, Pier Luigi Martelli, Rita Casadio, Florian

Boecker, Indika Kahanda, Natalie Thurlby, Alice McHardy, Alexandre Renaux, Rabie Saidi, Julian Gough, Alex Alves Freitas, Magdalena Antczak, Fábio Fabris, Mark N. Wass, Jie Hou, Jianlin Cheng, Zheng Wang, Alfonso E. Romero, Alberto Paccanaro, Haixuan Yang, Tatyana Goldberg, Chenguang Zhao, Liisa Holm, Petri Törönen, Alan Medlar, Elaine Zosa, Itamar Borukhov, Ilya B. Novikov, Angela D. Wilkins, Olivier Lichtarge, Po-Han Chi, Wei-Cheng Tseng, Michal Linial, Peter W. Rose, Christophe Dessimoz, Vedrana Vidulin, Sašo Džeroski, Ian P. W. Sillitoe, Sayoni Das, Jonathan G. Lees, David T. Jones, Cen Wan, Domenico Cozzetto, Rui Fa, Mateo Torres, Alex Warwick Vesztrocy, Jose Manuel Rodriguez, Michael L. Tress, Marco Frasca, Marco Notaro, Giuliano Grossi, Alessandro Petrini, Matteo Ré, Giorgio Valentini, Marco Mesiti, Daniel B. Roche, Jonas Reeb, David W. Ritchie, Sabeur Aridhi, Seyed Ziaeddin Alborzi, Marie-Dominique Devignes, Da Chen Emily Koo, Richard Bonneau, Vladimir Gligorijević, Meet Barot, Hai Fang, Stefano Toppo, Enrico Lavezzo, Marco Falda, Michele Berselli, Silvio C. E. Tosatto, Marco Carraro, Damiano Piovesan, Hafeez ur Rehman, Qizhong Mao, Shanshan Zhang, Slobodan Vucetic, Gage S Black, Dane Jo, Dallas J. Larsen, Ashton Omdahl, Luke Sagers, Erica Suh, Jonathan B. Dayton, Liam James McGuffin, Danielle Allison Brackenridge, Patricia C. Babbitt, Jeffrey M. Yunes, Paolo Fontana, Feng Zhang, Shanfeng Zhu, Ronghui You, Zihan Zhang, Suyang Dai, Shuwei Yao, Weidong Tian, Renzhi Cao, Caleb Chandler, Miguel Amezola, Devon Johnson, Jia-Ming Chang, Wen-Hung Liao, Yi-Wei Liu, Stefano Pascarelli, Yotam Frank, R. Hoehndorf, Maxat Kulmanov, Imane Boudellioua, Gianfranco Politano, Stefano Di Carlo, Alfredo Benso, Kai Hakala, Filip Ginter, Farrokh Mehryary, Suwisa Kaewphan, Jari Björne, Hans Moen, Martti Tolvanen, Tapiro Salakoski, Daisuke Kihara, Aashish Jain, Tomislav Šmuc, Adrian M. Altenhoff, Asa Ben-Hur, Burkhard Rost, Steven E. Brenner, Christine A. Orengo, Constance J. Jeffery, Giovanni Bosco, Deborah A. Hogan, Maria Jesus Martin, Claire O'Donovan, Sean D. Mooney, Casey S. Greene, Predrag Radivojac, and Iddo Friedberg. The CAFA challenge reports improved protein function prediction and new functional annotations for hundreds of genes through experimental screens. *Genome Biology*, 20, 2019.

Julia Zinkus-Boltz, Craig DeValk, and Bryan C. Dickinson. A Phage-Assisted Continuous Selection Approach for Deep Mutational Scanning of Protein–Protein Interactions. *ACS Chemical Biology*, 14(12):2757–2767, December 2019. ISSN 1554-8929, 1554-8937. doi: 10.1021/acscchembio.9b00669. URL <https://pubs.acs.org/doi/10.1021/acscchembio.9b00669>.

A Appendix

A.1 Social Impact

Protein design holds considerable promise for various fields, ranging from medicine to agriculture, and is likely to have a profound social impact. However, the development of such technology introduces several concerns, particularly relating to the dual use of protein fitness and design models. For instance, while beneficial for areas like drug design, these models can also be potentially utilized for harmful purposes such as bio-weapon design. Consider a generative model developed for therapeutic purposes: it typically penalizes predicted toxicity. Yet, the logic of this model could be inverted to instead reward for toxicity [Urbina et al., 2022]. Indeed, any tool or benchmark developed to improve protein design can be manipulated for nefarious objectives. Lastly, protein fitness models will significantly influence the way experiments are conducted. With increased adoption and development of protein design, substantial portions of experimental work can be accelerated, leading to quicker iterations and improved results. Nonetheless, the need for wet lab experimentation remains. These technological advancements will serve to augment, rather than completely supplant, traditional experimental procedures.

Additionally, the American College of Medical Genetics (ACMG) disregards computational prediction of variant effects due to insufficient validation. Consequently, it is essential to create benchmarks using clinical data in order to promote the acceptance of these machine learning methods in medical practice.

A.2 Limitations

Deep mutational scans While significant efforts have been dedicated to curating and preprocessing a diverse set of deep mutational scans (DMS), the very nature of these scans imposes biases and limitations to this benchmark:

1. **Measurement noise** Experiments do not have a perfect dynamic range, often imposing a restrictive ceiling and/or floor to the measured response of mutation effects that is not meaningful for protein function and mutation effect prediction. Furthermore, noise is a perennial issue in high-throughput assays, and some assays have poor experimental replicate correlation. Taken together, this means that one cannot expect perfect correlation between experiment and model. Since these considerations affect different proteins to different extents, computing average Spearman correlations across proteins can be misleading.
2. **Bias** There is additional bias in the types of proteins chosen for deep mutational scans. This can be due both to experimental limitations on which proteins' functions can be assayed (for example, disordered proteins are challenging), and to protein prioritisation considerations (for example, viral and cancer-related proteins are over-represented).
3. **Representativeness** No assay is fully representative of the impacts of protein changes on the evolutionary fitness of an organism, which typically involves a convolution of molecular functions across changing environments. In fact, many assays target only a single feature such as expression, binding, or enzymatic activity.
4. **Inconsistent processing** The reported fitness effects from DMS are themselves the result of modeling and analysis of the raw data. The treatment of data is extremely heterogeneous across the community and different analyses can lead to different conclusions on the effect of mutations. For a perfect standardised curation of experimental results one should treat all data with the same approach. We leave this type of analysis for future work.

Human mutation databases ClinVar data has the advantage of covering more proteins than DMS, even if only human proteins involved in disease. But it has several limitations:

1. **Noise** This dataset, by the very community-based nature of it, is very noisy. Filtering to more stringently curated ClinVar labels, or to more recent labels, improves correlation with predictions from sequence models [Frazer et al., 2021]. Here we decided to keep a reasonable number of clinical labels – a trade-off between quantity and quality.
2. **Bias** Clinical labels are biased towards classes of proteins that are heavily studied, such as well-known cancer genes, as well as towards European ancestry.
3. **Circularity** Grimm et al. [2015] details two types of circularity that hinder the evaluation of human variant effect predictors. In a supervised benchmark, there is the potential for data leakage from training to testing, even for different variants in the same protein. Even for our unsupervised benchmark, where models have not trained on clinical labels, there is the potential for another type of circularity: evolutionary conservation is one of the criteria used to classify a variant as benign or pathogenic in ClinVar.

Finally, the current benchmarks are limited to mutations in coding regions. But there are both DMS datasets and clinical labels (although fewer of them) in regulatory regions – for example in UTRs, introns, promoters. This could be an interesting direction of growth for these benchmarks.

A.3 Datasets

A.3.1 DMS assays

Evolution of protein fitness benchmarks based on DMS assays As discussed in § 2, our DMS benchmarks build on several prior works that had compiled a growing library of such assays. We summarize their content in Table A1.

Category	Mut. Type	Metric or Setting	EVmutation	Deep Sequence	ProteinGym v0.1	ProteinGym v1.0
DMS	Sub.	Assays (mut.)	26 (0.1M)	38 (0.7M)	87 (1.6M)	217 (2.4M)
	Ind.	Assays (mut.)	0 (0k)	0 (0k)	7 (270k)	66 (289k)
Clinical	Sub.	Genes (mut.)	0	0	0	2,525 (63k)
	Ind.	Genes (mut.)	0	0	0	1,555 (3k)
Training regime	Sub.	Zero-shot	✓	✓	✓	✓
	Ind.	Zero-shot	-	-	✓	✓
	Sub.	Supervised	-	-	-	✓
	Ind.	Supervised	-	-	-	✓
Baselines	Sub.	Zero-shot	5	3	9	42
	Ind.	Zero-shot	0	0	3	20
	Sub.	Supervised	0	0	0	9
	Ind.	Supervised	0	0	0	3
Metrics	-	Zero-shot	2	3	3	5
	-	Supervised	0	0	0	2

Table A1: **Evolution of protein fitness benchmarks** ProteinGym v0.1 corresponds to benchmarks in Notin et al. [2022a], while ProteinGym v1.0 corresponds to benchmarks in this paper. The EVmutation benchmark was introduced in Hopf et al. [2017], while the DeepSequence benchmark was developed in Riesselman et al. [2018]. Sub., Ind. and mut. are shorthands for substitutions, indels and mutants respectively.

Selection and processing We focused on several different criteria when determining which DMS assays to include in ProteinGym. These are:

1. The public availability of data
2. The experimental throughput (how many mutations were assayed)
3. The level of noise between experiment replicates
4. The dynamic range of the assay
5. The assay type (selection, enrichment, etc) and whether or not it captures evolutionary constraints.
6. If the assay used amino-acid substitution or indel mutations (no UTR, tRNA, promoter, etc. variants were included).

Final list of assays In-depth metadata about the assays, including the assay type, UniProt ID, MSA start and end positions, mutated positions, and target sequence, is provided under the `reference_files` directory in the codebase. A complete list of included assays is presented at the end of the appendix (See Tables A19 and A20)

Processing of large thermostability dataset A large dataset of thermostability assays of 331 natural domains [Tsuboyama et al., 2023] contributed 65 assays to our list. We processed these assays as follows:

We used the set of non-redundant natural domains (referred to as Dataset #5 in the original paper). After mapping to UniProt IDs for our DMS id naming convention and removing datasets where none of the tested evolutionary models had a Spearman correlation above 0.2 (suggesting that there is inadequate evolutionary fitness signal in the stability assay, preventing meaningful comparisons between models), we were left with 65 thermostability

Function type	# Assays		Description
	Subs	Indels	
Activity	43	3	Assays that directly or indirectly measure a protein's catalytic (or otherwise biochemical) activity
Binding	14	0	Assays that measure the affinity or the degree to which a protein binds its target
Expression	17	2	Assays that measure how much the protein is expressed in a cell
Organismal fitness	77	6	Assays that measure how much changes in the protein affect an organism's growth rate
Stability	66	55	Assays that measure how thermostable a protein is

Table A2: **DMS assay function types.** The number of substitution and indel assays in each of the 5 function type categories and a general description used to categorize the assays.

assays of short domains (40-72 residues long). For substitutions, there was 99% coverage of each position with 14-19 mutations per position (and 52 of those datasets with multiples), and for indels there was a deletion, Gly and Ala insertion at every position.

Classification of DMS assays We grouped the substitution DMS assays into five function types: activity, binding, expression, organismal fitness, and stability. While many DMS assays are well described by multiple classes, we assigned each to a primary class such that the classes are non-overlapping. We provide a brief description of each class in Table A2.

Cross-validation schemes As described in § 4.2, we leverage 3 types of cross validation schemes: 'Random', 'Contiguous' and 'Modulo'. We only keep single substitution mutants for the corresponding analyses. For the 'Random' split, we randomly assigned each mutant to one of 5 folds. The 'Contiguous' split is obtained by splitting the sequence in contiguous segments along its length, ensuring the segments are comprised of the same number of positions. The 'Modulo' scheme is obtained by assigning positions to each fold using the modulo of the position number by the total number of folds. Therefore, for a 5-fold cross validation, position 1 is assigned to fold 1, position 2 to fold 2, ..., position 6 to fold 1, etc. Once again, we make sure to only consider mutated positions. We operate a five fold cross validation for all assays except for assays F7YBW8_MESOW [Aakre et al., 2015] and SPG1_STRSG [Wu et al., 2016], as these contain only 4 mutated positions.

High-level statistics Table A3 describes the size and mutation depth of the indel datasets.

A.3.2 Clinical datasets

We collect 65k variants from the ClinVar and gnomAD databases (Table A4).

For our indel benchmark, detailed in Section 4.1, we focus on short indels, less than or equal to three amino acids, which make up over 80% of in-frame indels in our data. There were insufficient benign annotations for indel clinical variants, so gnomAD common variants (allele frequency > 0.5%) were used as a pseudocontrols.

ClinVar processing The clinical substitutions dataset was obtained following the procedure from EVE [Frazer et al., 2021], detailed in Supplementary Methods Section 3 of that paper (which dataset is downloadable from <https://evemode1.org/download/bulk>), but correcting for mapping errors to GRCh38, which yielded 2,525 proteins and 63k variants, with Pathogenic/Likely Pathogenic/Benign/Likely Benign annotations and at least 1 star of clinical evidence - where assertion criteria is provided by a submitter. As a result, our dataset contains significantly more mutants than the dataset from [Frazer et al., 2021] (42k vs. 63k).

The raw set of inframe indels was obtained from ClinVar on February 6th, 2023, by using the following query:

```
("inframe deletion" [Molecular consequence] OR "inframe indel" [Molecular consequence]
OR "inframe insertion" [Molecular consequence])
```

This query yielded 18407 variants. After filtering out invalid/uncertain amino acids, repeats, remaining frameshift variants, and synonymous/stop codons, 17039 (92.5%) remained.

When filtering for Benign/Pathogenic/Likely Benign/Likely Pathogenic annotations (80%+ of annotations are uncertain significance), and selecting variants in genes with at least one P/LP annotation, and filtering indels up to 3 amino acids, $2090 / 18407 = 11.35\%$ of the original variants remained, 330 benign and 1760 pathogenic. When using gnomAD as the benign pseudocontrols, we only keep the 1760 pathogenic variants from ClinVar.

Dataset	#Datapoints (Benign/Path.)	Mutation Depth (Min/Mean/Max)	Mutation Source
DMS Assays			
AAV	24,909	1/3.57/11	randomization
β -Lac	4,751	1/1/1	library
Kir2.1	10,502	1/1.2/3	library
MtrA	331	8/8/8	library
PTEN	314	1/1/1	library
TP53	341	1/1.5/2	library
amyloid β	2,354	1/14/39	library
OCT1	543	1/1/1	library
Tsuboyama	14,280	1/2.7/3	library
Assays of Natural and Designed Sequences			
AAV	225,998	3/13.9/37	model-designed
CM	3,074	1/68.9/82	model-designed
HIS3	6,102	1/8.4/29	interpolations between natural sequences
Human Variants			
ClinVar	3k (1,760 / 839)	1 / 1.37 / 3	population variation

Table A3: **Summary of indel datasets.**

Dataset	#Proteins	#Variants	#Variants per Protein (Median)
Substitutions	2,525	63k	6
Indels	1,555	3k	1

Table A4: **Summary of ClinVar human variant datasets.**

All the preprocessing code from raw ClinVar data is available in the companion codebase.

gnomAD processing The Genome Aggregation Database (gnomAD) [Karczewski et al., 2020] seeks to aggregate genome and exome sequencing data from multiple large-scale sequencing projects, and publishes summary data such as variant allele frequencies in a consistent format. The gnomAD v2.1.1 GRCh38 liftover was downloaded on February 8th 2023 and contains 125,748 exomes and 15,708 genomes. v2 was originally based on the GRCh37 reference sequence and v2.1.1 was lifted over to the GRCh38 reference sequence.

The inframe indels were similarly preprocessed to the ClinVar indels (the preprocessing code from raw data is also available in the repository), yielding 839 common indels up to 3 amino acids in length.

A.3.3 Access

The following provides more details on the code and data Resources (§ 6) accompanying this paper.

The open-source codebase containing a framework for scoring all the benchmarks (and easily facilitating the addition of new benchmarks) is available at <https://github.com/OATML-MarksLab/ProteinGym>. Modifications of certain baselines (e.g. scoring of long sequences beyond the context size in the ESM suite, or pre-processing of MSAs in MSA Transformer) are also released, and all of the model predictions can be reproduced using this repository. We also include preprocessing code for the clinical data (ClinVar/gnomAD) and DMS assays for reproducibility.

We developed a user-friendly website, <https://www.proteingym.org> containing a leaderboard, detailed results per assay, as well as drill analyses across various dimensions (e.g. mutational depth, taxa).

The DMS assays, model scores, Multiple Sequence Alignments, predicted 3D structures, processed ClinVar/gnomAD datasets, and raw files before preprocessing are made available at <https://marks.hms.harvard.edu/proteingym/>. Instructions for downloading are in the GitHub repository. Some model checkpoints and other files necessary for scoring (for baselines such as profileHMM, PROVEAN) are also available at the FTP server, although most model checkpoints such as ESM-1v are available from their respective repositories.

A.3.4 License

The codebase is open source under the MIT license.

A.4 Baselines

Unless otherwise specified, model scores are calculated by taking the log-ratio of the sequence probabilities between the mutant and wild-type sequences $\log \frac{p(\mathbf{x}_{\text{mut}})}{p(\mathbf{x}_{\text{wt}})}$, following the convention in Hopf et al. [2017].

A.4.1 Zero-shot baselines

Alignment-based models

- **Site-independent Model** We use a site-wise maximum entropy model to infer the contribution of site-specific amino acid constraints without considering explicit epistatic constraints. This model is implemented as referred to in Hopf et al. [2017].
- **HMM** We use the profile hidden Markov model (HMM) implementation in HMMER [Eddy, 2011]. Profile HMMs are frequently used to generate multiple sequence alignments, but also produce log probabilities of sequences that can be used as estimates of fitness for both substitutions and indels [Durbin et al., 1998].
- **EVMutation** EVMutation [Hopf et al., 2017] models pairwise evolutionary couplings between protein sequences using a Potts model (otherwise known as a Markov Random Field).
- **DeepSequence** DeepSequence [Riesselman et al., 2018] uses a VAE architecture to learn higher-order non-linear evolutionary constraints within each protein family. Mutation effect scores are calculated similarly as EVMutation, as the log-ratio between the mutant and wild-type sequence probabilities $\log \frac{p(\mathbf{x}_{\text{mut}}|\theta)}{p(\mathbf{x}_{\text{wt}}|\theta)}$, but using the VAE evidence lower bound (ELBO) as a proxy for $p(\mathbf{x}|\theta)$.
- **WaveNet** We use a previously published dilated convolutional neural network (dilCNN) based on the WaveNet architecture [Shin et al., 2021] as an example of a family-specific sequence decoder capable of handling indels. Due to the expense of training a separate model for each protein, we only evaluate this model against the DMS datasets. Sequence scores are calculated as the difference in (length-normalized) log-likelihoods between the mutant and wild-type sequences.
- **EVE** EVE [Frazer et al., 2021] is a Bayesian VAE model architecture for predicting clinical variant effects. The model includes a Gaussian Mixture Model fitted to the background distribution of mutations, in order to provide interpretable protein-specific pathogenicity scores. We use the ClinVar preprocessing pipeline from EVE, and EVE is also used in TranceptEVE [Notin et al., 2022b].
- **GEMME** GEMME is the Global Epistatic Model for predicting Mutational Effects. It infers the conservation of combinations of mutations across the entire sequence according to an evolutionary tree [Engelen et al., 2009] and combines it with site-wise frequencies to calculate a combined epistatic sequence score for mutations [Laine et al., 2019]. GEMME intakes multiple sequence alignments of protein families as well as specific mutations to generate scores. To obtain scores, we used the GEMME web-tool hosted at <http://www.1cqb.upmc.fr/GEMME/submit.html> with default parameters.

Protein language models Protein language models are so called because they all use variants of the Transformer [Vaswani et al., 2017] architecture popularised in natural language processing.

- **UniRep** UniRep [Alley et al., 2019b] trains a Long Short-Term Memory (LSTM) model on UniRef50 [Suzek et al., 2015] sequences. It learns how to internally represent proteins by being trained on next amino acid prediction through minimizing cross-entropy loss. While the core model is trained on unaligned sequences, UniRep can also be fine-tuned on sets of homologous sequences from a given family, retrieved with a MSA. This process is called ‘evotuning’ and typically leads to stronger fitness prediction performance.
- **ESM** ESM-1b [Rives et al., 2021] and ESM-1v [Meier et al., 2021] are protein language models with a Transformer encoder architecture similar to BERT [Devlin et al., 2019] and trained with a Masked-Language Modeling (MLM) objective on UniRef50 and UniRef90 respectively. We extend the original ESM codebase for these two models to handle sequences that are longer than the model context window (ie., 1023 amino acids), with the approach described in Brandes et al. [2023] for ESM-1b and in Notin et al. [2022a] for ESM-1v. We predict fitness for ESM models with the masked-marginal approach introduced in Meier et al. [2021], which provides optimal performance on substitutions, but does not support indels.
- **CARP** CARP [Yang et al., 2023a] is a protein language model trained with a MLM objective on UniRef50. The architecture leverages convolutions instead of self-attention, leading to computational speedups while maintaining high downstream task performance.

- **RITA** RITA [Hesslow et al., 2022] is an autoregressive language model akin to GPT2 [Radford et al., 2019], trained on UniRef100 [Suzek et al., 2015]. Four model sizes are available, ranging from 85 million to 1.2 billion parameters. RITA takes unaligned sequences as input, and can score both substitution and indel mutations.
- **ProGen2** ProGen2 [Nijkamp et al., 2022] is an autoregressive protein language model trained on a mixture of UniRef90 [Suzek et al., 2014] and BFD30 [Steinegger and Söding, 2018]. It follows the standard transformer decoder architecture, and five models of different sizes are available, ranging from 151 million to 6.4 billion parameters. ProGen2 takes unaligned sequences as input, and can score both indel and substitution mutations.
- **VESPA** VESPA [Marquet et al., 2022] is as Single Amino acid Variant (SAV) effect predictor based on a combination the embeddings from the protein language model ProtT5 [Elnaggar et al., 2021], as well as per-residue conservation predictions.

Inverse Folding models Inverse folding models learn the conditional distribution of sequences that are likely to fold to an input protein structure [Ingraham et al., 2019]. Given that there may not be experimentally solved structures for the target sequence of all DMS assays in ProteinGym, we generate input structures using AlphaFold2 (AF2) [Jumper et al., 2021]. The inverse folding model in combination with AF2 encompasses an end-to-end scoring pipeline that only requires a protein sequence to score variants. As the sequence representation size is defined by the size of the input structure, the models we benchmark here can only score substitutions.

- **ProteinMPNN** ProteinMPNN [Dauparas et al., 2022] takes in a protein backbone structure and featurizes it as a graph where backbone (N,C,C α) atoms are nodes and edges are determined via euclidian distance cut-offs. The model uses a message passing neural network (MPNN) [Ingraham et al., 2019] to encode the structure into a latent graph representation. The model then decodes the representation and samples sequences autoregressively.
- **MIF** The Masked Inverse Folding (MIF) and Masked Inverse Folding with Sequence Transfer (MIF-ST) models [Yang et al., 2023b] are structured-conditioned protein language models trained with a MLM objective. MIF is trained on CATH4.2 [Dawson et al., 2016], and MIF-ST further augments the MIF model with embeddings from CARP (640M).
- **ESM-IF1** ESM-IF1 [Hsu et al., 2022b] functions similarly to ProteinMPNN but leverages a Geometric Vector Perceptron [Jing et al., 2020] (an equivariant message passing module ideal for coordinate data) as the architecture for the structure encoder and sequence decoder.

Hybrid models

- **MSA Transformer** The MSA Transformer [Rao et al., 2021] learns a representation of Multiple Sequence Alignments (MSAs) by training an Axial transformer-based transformer [Ho et al., 2019a] with a MLM objective across a diverse set of 26 million MSAs.
- **Tranception** Tranception [Notin et al., 2022a] combines an autoregressive protein language model with inference-time retrieval from a MSA. We evaluate Tranception Small (85M), Tranception Medium (300M parameters) and Tranception Large (700M parameters) both with and without MSA retrieval. Tranception can score both indel and substitution mutations.
- **TranceptEVE** TranceptEVE augments Tranception with priors for the amino acid distribution at each position based on an ensemble of EVE models for the protein family of interest. The final output log probability is thus a weighted sum of that EVE log prior, the log probability from the autoregressive transformer model in Tranception, as well as site-specific log probabilities obtained from a retrieved MSA (as in the inference-time retrieval procedure described in Tranception). TranceptEVE can score both indels and substitutions.

A.4.2 Supervised baselines

We leverage the various supervised baselines defined in Notin et al. [2023]:

- **One-hot encoding (OHE) models** OHE baselines take as input a one-hot encoding representation of the amino acid sequence, together with zero-shot fitness predictions obtained with several of the baselines discussed above in Appendix A.4.1. Both are input into a L2-penalized regression, following the approach discussed in [Hsu et al., 2022a];
- **Embeddings models** Embeddings models are based on mean-pooled embeddings from various protein language models introduced above (e.g., Tranception, ESM-1v, MSA Transformer), augmented with zero-shot fitness predictions from the same model. We refer to Notin et al. [2023] for all implementation details;

- **ProteinNPT** ProteinNPT [Notin et al., 2023] is a semi-supervised non-parametric transformer [Kossen et al., 2022] which learns a joint representation of full batches of labeled sequences. It is trained with a hybrid objective consisting of fitness prediction and masked amino acids reconstruction. The model can be used to predict mutation effects for single or multiple properties simultaneously, and sample novel sequences conditioned on label values of interest.

A.4.3 Clinical baselines

We leverage a set of clinical variant effect predictors from dbNSFP v4.4a [Liu et al., 2011, 2020], which is a database of functional predictions for all possible non-synonymous single-nucleotide variants (nsSNVs) in the human genome.

These models were developed primarily to assess the effects of mutations in humans and are included in clinical benchmarks only:

- **Supervised** The following assays used ClinVar label annotations in their training (or are meta-predictors that contain one or more supervised models): ClinPred [Alirezaie et al., 2018], MetaRNN [Li et al., 2022], BayesDel [Feng, 2017], VEST4 (variant effect scoring tool 4.0) [Carter et al., 2013], REVEL [Ioannidis et al., 2016], VARIETY [Wu et al., 2021], gMVP [Zhang et al., 2022], CADD [Renzsch et al., 2019], PolyPhen2 [Adzhubei et al., 2010], DEOGEN2 [Raimondi et al., 2017], MPC [Samocha et al., 2017], MutationTaster [Schwarz et al., 2010], DANN [Quang et al., 2015], FATHMM[Shihab et al., 2013]
- **Unsupervised** In addition to TranceptEVE, GEMME, EVE and ESM-1b (zero-shot baselines mentioned above), the following unsupervised clinical variant effect predictors were used as baselines: PROVEAN [Choi et al., 2012], SIFT [Ng and Henikoff, 2002], MutationAssessor [Reva et al., 2011], MutPred [Li et al., 2009], PrimateAI [Sundaram et al., 2018], LIST-S2 [Malhis et al., 2020], and LRT [Chun and Fay, 2009].

For ESM-1b, we downloaded precomputed scores from [Brandes and Ntranos, 2023] from a recent study that extended ESM-1b to predict all possible missense variant effects in the human genome [Brandes et al., 2023]. TranceptEVE and EVE models were trained for the subset of 2,525 proteins in the clinical benchmark, and the model weights/scores are provided online for further analysis (See Section A.3.3). GEMME scores were obtained as detailed above. We provide an analysis of performance on clinical datasets vs the subset of assays on human proteins in Fig. 2.

A.5 Detailed performance results

A.5.1 DMS substitution benchmarks

Zero-shot Table A5 shows the results for our zero-shot DMS substitutions benchmark. We report Spearman’s rank correlations and bootstrapped standard error estimates for forty baseline models. Table A6 breaks down our substitution DMS by MSA depth, Table A7 by function type, Table A8 by taxa, and Table A9 by mutational depth. To compute the final Spearman’s rank correlation reported in Table A5, we first average all the assays for a particular function type together, resulting in five average values (one each for Activity, Binding, Expression, Organismal Fitness, and Stability). The average of these five numbers is the final reported value.

Clustering zero-shot substitution models We clustered the zero-shot models using hierarchical clustering on the vector of NDCG metrics for each dataset in the DMS substitutions (Fig. A1). We find that models with the same architecture tend to cluster together (e.g., RITA models), however, there are exceptions (e.g., ESM-2 models). We also observe that the alignment-based models tend to cluster together, suggesting that training on the same MSA may promote similar scoring behavior.

Supervised Table A10 shows the results for our supervised DMS substitutions benchmark. We report Spearman’s rank correlations for 10 baseline models.

A.5.2 DMS indel benchmarks

Zero-shot Table A14 shows the results for our zero-shot DMS indels benchmark, and Table A15 shows Spearman’s rank correlations for each indel DMS dataset and model. Figure A2 compares each model’s aggregate performance between the Library and Designed DMS sets (numbers provided in Table 4). More detailed performance files are available in the repository.

Supervised Table A16 ranks the performance of each model on the supervised indel DMS benchmark.

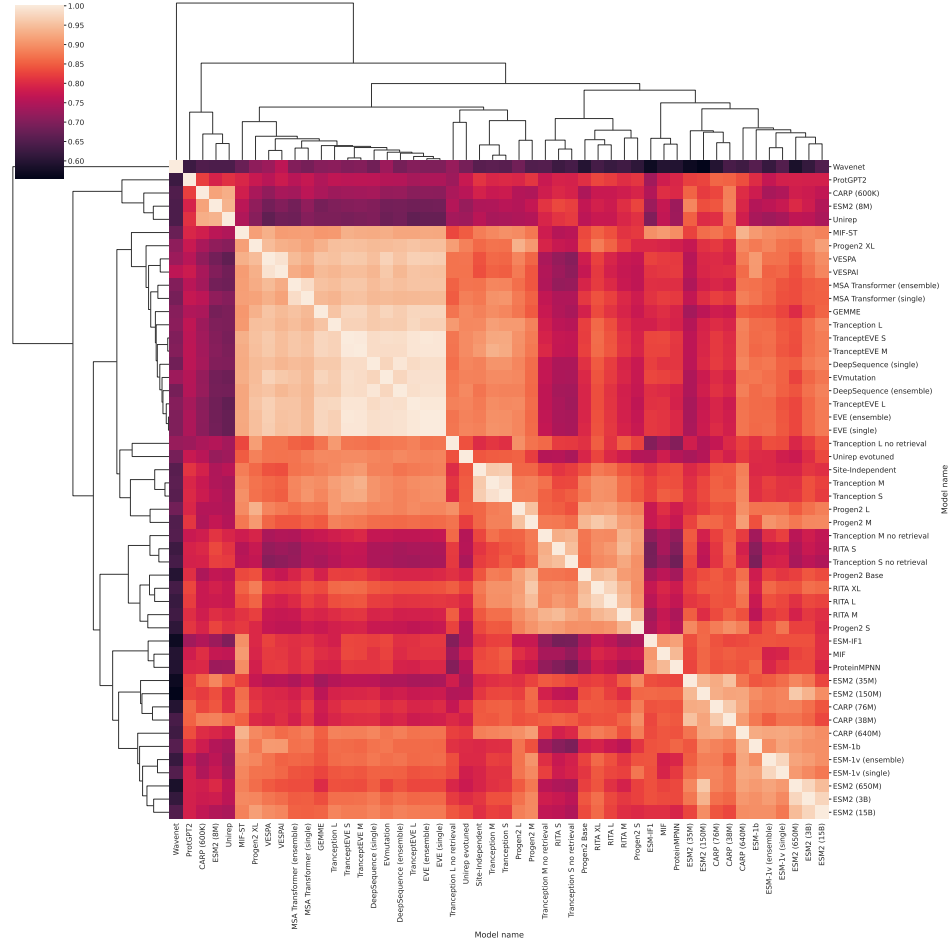


Figure A1: Hierarchical clustering of zero-shot models by NDCG performance Heatmap colored by the Pearson correlation of the NDCG@10% values for each DMS assay for each pair of zero-shot models. Lighter color corresponds to higher correlation. The ordering and dendrogram were produced by hierarchical clustering of the correlation values.

A.5.3 Clinical substitution benchmarks

As discussed in § 4, since the performance of zero-shot models is on par – or higher – than their supervised counterparts we subsume the Clinical zero-shot and supervised rankings into a combined rankings, available in Table A17. Although supervised models trained on ClinVar labels (such as ClinPred) perform well on the clinical benchmark, unsupervised models (such as TranceptEVE) provide better performance on the subset of DMS assays assessing the clinical effect of variants in humans, and competitive performance on the clinical benchmark without being subject to the same label biases (see Fig. 2).

A.5.4 Clinical indel benchmarks

Table A18 shows model performance on the ClinVar datasets, and Figure A3 shows the combined performance on the DMS and ClinVar indel benchmarks.

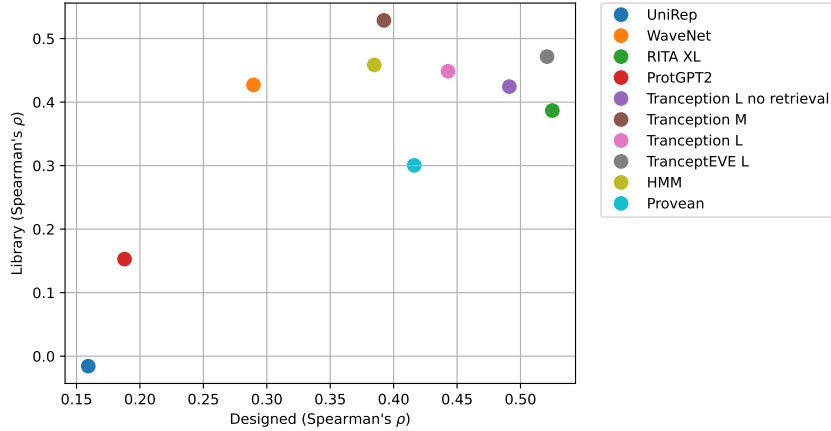


Figure A2: **Performance comparison of indel baselines on different types of assays** Spearman's rank correlation over unbiased libraries vs model-designed sequences biased towards natural sequences.

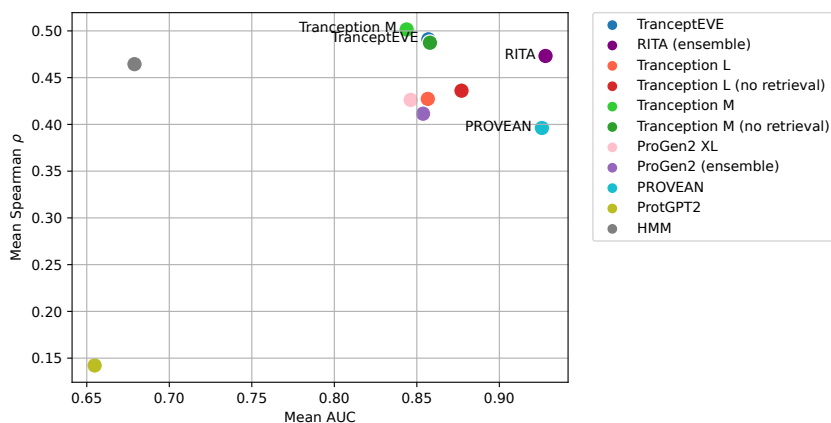


Figure A3: **Performance comparison of indel baselines on the indel benchmarks.** AUC over ClinVar with gnomAD controls (x axis) and Spearman's rank correlation over functional assay benchmarks (y axis).

Ranking	Model	Type	Spearman	Std. error
1*	TranceptEVE L	Hybrid model	0.457	0.000
1*	GEMME	Alignment-based model	0.457	0.007
3	TranceptEVE M	Hybrid model	0.456	0.004
4	TranceptEVE S	Hybrid model	0.453	0.004
5	EVE (ensemble)	Alignment-based model	0.441	0.006
6	VESPA	Protein language model	0.437	0.006
7	Tranception L	Hybrid model	0.436	0.003
8	EVE (single)	Alignment-based model	0.434	0.005
9	MSA Transformer (ensemble)	Hybrid model	0.434	0.009
10	Tranception M	Hybrid model	0.429	0.005
11	ESM-IF1	Inverse folding model	0.422	0.012
12	DeepSequence (ensemble)	Alignment-based model	0.422	0.008
13	MSA Transformer (single)	Hybrid model	0.421	0.009
14	Tranception S	Hybrid model	0.419	0.006
15	ESM-2 (650M)	Protein language model	0.419	0.011
16	ESM-1v (ensemble)	Protein language model	0.416	0.011
17	DeepSequence (single)	Alignment-based model	0.411	0.008
18	ESM-2 (3B)	Protein language model	0.410	0.010
19	ESM-2 (15B)	Protein language model	0.405	0.010
20	MIF-ST	Inverse folding model	0.401	0.010
21	ESM-1b	Protein language model	0.399	0.010
22	EVmutation	Alignment-based model	0.397	0.006
23	VESPA1	Protein language model	0.393	0.007
24	ProGen2 XL	Protein language model	0.392	0.008
25	ESM-2 (150M)	Protein language model	0.392	0.012
26	ESM-1v (single)	Protein language model	0.385	0.012
27	MIF	Inverse folding model	0.381	0.011
28	ProGen2 L	Protein language model	0.381	0.008
29	ProGen2 M	Protein language model	0.380	0.008
30	ProGen2 Base	Protein language model	0.379	0.009
31	Tranception L no retrieval	Protein language model	0.375	0.008
32	CARP (640M)	Protein language model	0.373	0.011
33	RITA XL	Protein language model	0.373	0.009
34	RITA L	Protein language model	0.366	0.009
35	Site-Independent	Alignment-based model	0.361	0.010
36	RITA M	Protein language model	0.350	0.010
37	Tranception M no retrieval	Protein language model	0.349	0.009
38	UniRep evotuned	Hybrid model	0.347	0.009
39	ProGen2 S	Protein language model	0.336	0.011
40	CARP (76M)	Protein language model	0.332	0.012
41	ESM-2 (35M)	Protein language model	0.325	0.014
42	RITA S	Protein language model	0.304	0.012
43	Tranception S no retrieval	Protein language model	0.303	0.012
44	CARP (38M)	Protein language model	0.283	0.013
45	ProteinMPNN	Inverse folding model	0.258	0.011
46	ESM-2 (8M)	Protein language model	0.229	0.015
47	WaveNet	Alignment-based model	0.216	0.017
48	UniRep	Protein language model	0.193	0.016
49	ProtGPT2	Protein language model	0.188	0.011
50	CARP (600K)	Protein language model	0.108	0.017

Table A5: **ProteinGym - Zero-shot substitution DMS benchmark** Ranking based on Spearman's rank correlation between experimental assay measurement and model prediction. The standard error reported corresponds to the non-parametric bootstrap standard error of the difference between the Spearman performance of a given model and that of the best overall model (i.e., TranceptEVE), computed over 10k bootstrap samples from the set of proteins in the ProteinGym DMS substitution benchmark.

Model type	Model name	Spearman by MSA depth (↑)			
		Low	Medium	High	All
Alignment-based	Site-Independent	0.426	0.373	0.320	0.373
	WaveNet	0.207	0.255	0.207	0.223
	EVmutation	0.403	0.423	0.410	0.412
	DeepSequence (ens.)	0.383	0.428	0.473	0.428
	EVE (ens.)	0.425	0.453	0.481	0.453
	GEMME	0.455	0.470	0.497	0.474
Protein language	UniRep	0.181	0.161	0.209	0.184
	CARP (640M)	0.314	0.375	0.428	0.372
	ESM-1b	0.350	0.398	0.482	0.410
	ESM-2 (15B)	0.357	0.414	0.473	0.415
	RITA XL	0.315	0.382	0.412	0.370
	ESM-1v (ens.)	0.326	0.418	0.502	0.415
	ProGen2 XL	0.354	0.405	0.444	0.401
	VESPA	0.427	0.455	0.484	0.455
Hybrid	UniRep evotuned	0.330	0.344	0.372	0.349
	MSA Transformer (ens.)	0.404	0.450	0.488	0.447
	Tranception L	0.432	0.438	0.473	0.448
	TranceptEVE L	0.451	0.467	0.492	0.470
Inverse Folding	ESM-IF1	0.300	0.431	0.544	0.425
	MIF-ST	0.376	0.403	0.456	0.412
	ProteinMPNN	0.173	0.280	0.434	0.296

Table A6: **ProteinGym - Zero-shot substitution DMS benchmark by MSA depth** Average Spearman's rank correlation between model scores and experimental measurements by MSA depth on the ProteinGym substitution benchmark. Alignment depth is measured by the ratio of the effective number of sequences N_{eff} in the MSA, following Hopf et al. [2017], by the length covered L (Low: $N_{\text{eff}}/L < 1$; Medium: $1 < N_{\text{eff}}/L < 100$; High: $N_{\text{eff}}/L > 100$). The All column is the average across the 3 depths.

Model type	Model name	Spearman by Function Type (↑)					
		Activity	Binding	Expression	Organismal Fitness	Stability	All
Alignment-based	Site-Independent	0.369	0.345	0.351	0.382	0.358	0.361
	WaveNet	0.219	0.187	0.185	0.303	0.182	0.215
	EVmutation	0.440	0.322	0.382	0.411	0.430	0.397
	DeepSequence (ens.)	0.455	0.368	0.396	0.413	0.476	0.422
	EVE (ens.)	0.464	0.394	0.406	0.447	0.491	0.440
	GEMME	0.482	0.387	0.443	0.452	0.519	0.457
Protein language	UniRep	0.182	0.203	0.230	0.141	0.210	0.193
	CARP (640M)	0.395	0.274	0.419	0.364	0.414	0.373
	ESM-1b	0.428	0.289	0.427	0.351	0.500	0.399
	ESM-2 (15B)	0.405	0.318	0.425	0.388	0.488	0.405
	RITA XL	0.366	0.303	0.416	0.381	0.398	0.373
	ESM-1v (ens.)	0.414	0.320	0.456	0.387	0.500	0.415
	ProGen2 XL	0.402	0.302	0.423	0.387	0.445	0.392
Hybrid	VESPA	0.468	0.365	0.410	0.440	0.500	0.437
	UniRep evotuned	0.355	0.304	0.366	0.346	0.366	0.347
	MSA Transformer (ens.)	0.469	0.343	0.439	0.421	0.495	0.433
	Tranception L	0.465	0.351	0.455	0.436	0.471	0.436
Inverse Folding	TranceptEVE L	0.487	0.381	0.456	0.460	0.500	0.457
	ESM-IF1	0.368	0.392	0.403	0.324	0.624	0.422
	MIF-ST	0.390	0.323	0.432	0.373	0.486	0.401
ProteinMPNN	ProteinMPNN	0.197	0.165	0.198	0.165	0.566	0.258

Table A7: **ProteinGym - Zero-shot substitution DMS benchmark by function type** Average Spearman's rank correlation between model scores and experimental measurements on the ProteinGym substitution benchmark, separated into five functional categories (Activity, Binding, Organismal Fitness, Stability and Expression). 'All' is the average of all the categories.

Model type	Model name	Spearman by Taxa (↑)				
		Human	Other Eukaryote	Prokaryote	Virus	All
Alignment-based	Site-Independent	0.379	0.385	0.316	0.383	0.366
	WaveNet	0.145	0.305	0.293	0.283	0.256
	EVmutation	0.409	0.444	0.422	0.388	0.416
	DeepSequence (ens.)	0.442	0.469	0.460	0.344	0.429
	EVE (ens.)	0.453	0.487	0.468	0.428	0.459
	GEMME	0.468	0.510	0.473	0.469	0.480
Protein language	UniRep	0.213	0.219	0.165	0.057	0.164
	CARP (640M)	0.416	0.386	0.390	0.273	0.366
	ESM-1b	0.434	0.475	0.455	0.241	0.401
	ESM-2 (15B)	0.431	0.449	0.459	0.313	0.413
	RITA XL	0.394	0.384	0.353	0.402	0.383
	ESM-1v (ens.)	0.458	0.446	0.454	0.289	0.412
	ProGen2 XL	0.384	0.442	0.439	0.391	0.414
Hybrid	VESPA	0.438	0.492	0.490	0.432	0.463
	UniRep evotuned	0.355	0.363	0.346	0.349	0.353
	MSA Transformer (ens.)	0.437	0.505	0.463	0.414	0.455
	Tranception L	0.453	0.483	0.431	0.432	0.450
Inverse Folding	TranceptEVE L	0.471	0.498	0.473	0.453	0.474
	ESM-IF1	0.415	0.497	0.507	0.374	0.448
	MIF-ST	0.404	0.415	0.463	0.396	0.420
ProteinMPNN	ProteinMPNN	0.282	0.395	0.354	0.248	0.320

Table A8: **ProteinGym - Zero-shot substitution DMS benchmark by taxa** Average Spearman's rank correlation between model scores and experimental measurements on the ProteinGym substitution benchmark, separated by taxon. 'All' is the average across the taxa.

Model type	Model name	Spearman by Mutational Depth (↑)					
		1	2	3	4	5+	All
Alignment-based	Site-Independent	0.336	0.235	0.226	0.267	0.350	0.283
	WaveNet	0.176	0.059	0.218	0.181	0.258	0.178
	EVmutation	0.376	0.274	0.324	0.301	0.394	0.334
	DeepSequence (ens.)	0.405	0.264	0.313	0.309	0.378	0.334
	EVE (ens.)	0.428	0.273	0.308	0.298	0.355	0.332
	GEMME	0.447	0.274	0.321	0.324	0.414	0.356
Protein language	UniRep	0.175	0.071	0.111	0.141	0.191	0.138
	CARP (640M)	0.390	0.213	0.187	0.164	0.162	0.223
	ESM-1b	0.384	0.227	0.187	0.149	0.270	0.243
	ESM-2 (15B)	0.407	0.204	0.239	0.172	0.234	0.251
	RITA XL	0.356	0.139	0.136	0.154	0.233	0.204
	ESM-1v (ens.)	0.403	0.221	0.186	0.151	0.203	0.233
	ProGen2 XL	0.385	0.184	0.280	0.219	0.280	0.270
	VESPA	0.434	0.183	0.357	0.302	0.328	0.321
Hybrid	UniRep evotuned	0.319	0.154	0.250	0.226	0.294	0.249
	MSA Transformer (ens.)	0.426	0.238	0.384	0.366	0.408	0.364
	Tranception L	0.423	0.258	0.352	0.318	0.387	0.348
	TranceptEVE L	0.446	0.280	0.350	0.320	0.382	0.356
Inverse Folding	ESM-IF1	0.439	0.345	0.290	0.289	0.358	0.344
	MIF-ST	0.430	0.265	0.334	0.298	0.298	0.325
	ProteinMPNN	0.292	0.257	0.171	0.186	0.278	0.237

Table A9: **ProteinGym - Zero-shot substitution DMS benchmark by mutational depth** Average Spearman's rank correlation between model scores and experimental measurements on the ProteinGym substitution benchmark, separated by mutational depths of 1,2,3,4, and 5 or more. The All column is the average across the 5 depths.

Ranking	Model name	Model type	Spearman
1	ProteinNPT	NPT	0.613
2	Tranception	Embeddings	0.571
3	MSA Transformer	Embeddings	0.568
4	ESM-1v	Embeddings	0.542
5	TranceptEVE	OHE	0.477
6	Tranception	OHE	0.458
7	MSAT	OHE	0.453
8	DeepSequence	OHE	0.440
9	ESM-1v	OHE	0.417
10	OHE w/o augmentation	OHE	0.224

Table A10: **ProteinGym - Supervised substitution DMS benchmark** Ranking based on Spearman's rank correlation between experimental assay measurement and model prediction.

Model type	Model name	Spearman by MSA depth (↑)			
		Low	Medium	High	All
NPT	ProteinNPT	0.701	0.587	0.608	0.632
Embeddings	Tranception	0.621	0.556	0.561	0.579
	MSAT	0.685	0.518	0.567	0.590
	ESM-1v	0.653	0.465	0.541	0.553
One-hot encoding	TranceptEVE	0.503	0.483	0.468	0.485
	Tranception	0.490	0.455	0.445	0.463
	MSAT	0.500	0.441	0.448	0.463
	DeepSequence	0.482	0.422	0.426	0.443
	ESM-1v	0.496	0.338	0.400	0.411
	No Augmentation	0.246	0.204	0.227	0.226

Table A11: **Supervised substitution DMS benchmark by MSA depth** Average Spearman’s rank correlation between model scores and experimental measurements by MSA depth on the ProteinGym substitution benchmark. Alignment depth is measured by the ratio of the effective number of sequences N_{eff} in the MSA, following Hopf et al. [2017], by the length covered L (Low: $N_{\text{eff}}/L < 1$; Medium: $1 < N_{\text{eff}}/L < 100$; High: $N_{\text{eff}}/L > 100$)

Model type	Model name	Spearman by Function Type (↑)				
		Activity	Binding	Expression	Organismal Fitness	Stability
NPT	ProteinNPT	0.577	0.536	0.637	0.545	0.772
Embeddings	Tranception	0.520	0.529	0.613	0.519	0.674
	MSAT	0.547	0.470	0.584	0.493	0.749
	ESM-1v	0.487	0.450	0.587	0.468	0.717
One-hot encoding	TranceptEVE	0.502	0.444	0.476	0.470	0.493
	Tranception	0.475	0.416	0.476	0.448	0.473
	MSAT	0.480	0.393	0.463	0.437	0.491
	DeepSequence	0.467	0.418	0.424	0.422	0.471
	ESM-1v	0.421	0.363	0.452	0.383	0.463
	No Augmentation	0.213	0.212	0.226	0.194	0.273

Table A12: **Supervised substitution DMS benchmark by function type** Average Spearman’s rank correlation between supervised model scores and experimental measurements on the ProteinGym substitution benchmark, separated into five functional categories. Assays are split into one of Activity, Binding, Organismal Fitness, Stability and Expression. The All column is the average of all the categories

Model type	Model name	Spearman by Taxa (↑)				
		Human	Other Eukaryote	Prokaryote	Virus	All
NPT	ProteinNPT	0.649	0.628	0.668	0.580	0.631
Embeddings	Tranception	0.569	0.582	0.594	0.568	0.578
	MSAT	0.634	0.579	0.648	0.521	0.596
	ESM-1v	0.565	0.579	0.617	0.433	0.548
One-hot encoding	TranceptEVE	0.481	0.490	0.475	0.478	0.481
	Tranception	0.457	0.472	0.453	0.456	0.460
	MSAT	0.482	0.459	0.468	0.448	0.464
	DeepSequence	0.451	0.460	0.455	0.383	0.437
	ESM-1v	0.426	0.444	0.452	0.292	0.404
	No Augmentation	0.236	0.217	0.233	0.238	0.231

Table A13: **Supervised substitution DMS benchmark by taxa** Average Spearman’s rank correlation between model scores and experimental measurements on the ProteinGym substitution benchmark, separated into four taxon categories. Assays are split into one of Human, Prokaryote, Other Eukaryote, or Virus. The All column is the average across the categories.

Ranking	Model	Type	Spearman	Std. error
1*	TranceptEVE M	Hybrid model	0.467	0.000
1*	ProGen2 M	Protein language model	0.467	0.054
3	ProGen2 Base	Protein language model	0.466	0.051
4	RITA L	Protein language model	0.459	0.039
5	TranceptEVE L	Hybrid model	0.457	0.014
6	Tranception M no retrieval	Protein language model	0.455	0.045
7	RITA XL	Protein language model	0.452	0.038
8	ProGen2 L	Protein language model	0.451	0.049
9	Tranception L no retrieval	Protein language model	0.439	0.040
10	RITA M	Protein language model	0.439	0.032
11	ProGen2 XL	Protein language model	0.434	0.029
12	ProGen2 S	Protein language model	0.425	0.049
13	Tranception S no retrieval	Protein language model	0.412	0.045
14	Tranception L	Hybrid model	0.399	0.032
15	RITA S	Protein language model	0.399	0.036
16	Tranception M	Hybrid model	0.398	0.029
17	Hidden Markov Model	Alignment-based model	0.391	0.028
18	TranceptEVE S	Hybrid model	0.361	0.032
19	PROVEAN	Alignment-based model	0.351	0.029
20	Tranception S	Hybrid model	0.344	0.031
21	WaveNet	Alignment-based model	0.285	0.046
22	ProtGPT2	Protein language model	0.194	0.033
23	UniRep	Protein language model	0.169	0.061

Table A14: **ProteinGym - Zero-shot indel DMS benchmark** Ranking based on Spearman’s rank correlation between experimental assay measurement and model prediction. The standard error reported corresponds to the non-parametric bootstrap standard error of the difference between the Spearman performance of a given model and that of the best overall model (ie., TranceptEVE), computed over 10k bootstrap samples from the set of proteins in the ProteinGym DMS indel benchmark.

Dataset	Tranception				ProGen2		PROVEAN	HMM	WaveNet
	M	L	M+Ret	L+Ret	M	XLarge			
DMS Assays									
AAV	0.126	0.210	0.371	0.338	-0.100	0.167	0.177	0.057	-0.007
β -Lac	0.379	0.296	0.365	0.344	0.619	0.409	0.385	0.347	0.437
KCNJ2	0.412	0.391	0.437	0.440	0.432	0.386	0.386	0.368	0.408
MtrA	0.615	0.375	0.612	0.395	0.403	0.348	0.278	0.472	0.244
PTEN	0.700	0.563	0.678	0.546	0.552	0.402	0.237	0.668	0.697
TP53	0.579	0.395	0.536	0.362	0.428	0.354	0.273	0.482	0.031
Assays of Natural and Designed Sequences									
AAV	0.362	0.691	0.677	0.709	-0.466	0.492	0.683	0.607	0.666
CM	0.219	0.223	0.344	0.326	0.380	0.379	0.372	0.398	0.438
HIS3	0.687	0.707	0.611	0.655	0.702	0.713	0.701	0.548	0.687

Table A15: **Spearman's rank correlation between model scores and individual deep mutational scans of indels.**

Ranking	Model	Type	Spearman
1	ESM-1v	Embeddings	0.752
2	Tranception	Embeddings	0.735
3	MSAT	Embeddings	0.689

Table A16: **ProteinGym - Supervised indel DMS benchmark** Ranking based on Spearman's rank correlation between experimental assay measurement and model prediction.

Ranking	Model	Type	AUC
1	ClinPred	Supervised	0.981
2	MetaRNN	Supervised	0.977
3	BayesDel (addAF)	Supervised	0.972
4	VEST4	Supervised	0.929
5	REVEL	Supervised	0.928
6	BayesDel (noAF)	Supervised	0.925
7	VARIETY (R)	Supervised	0.921
8	TranceptEVE	Unsupervised	0.920
9	GEMME	Unsupervised	0.919
10	VARIETY (ER)	Supervised	0.918
11	EVE	Unsupervised	0.917
12	gMVP	Supervised	0.914
13	CADD	Supervised	0.905
14	PolyPhen2 (HVAR)	Supervised	0.896
15	DEOGEN2	Supervised	0.894
16	ESM-1b	Unsupervised	0.892
17	PROVEAN	Unsupervised	0.886
18	MPC	Supervised	0.881
19	PolyPhen2 (HDIV)	Supervised	0.879
20	SIFT	Unsupervised	0.878
21	SIFT4G	Unsupervised	0.877
22	MutationAssessor	Unsupervised	0.877
23	MutPred	Unsupervised	0.875
24	PrimateAI	Unsupervised	0.855
25	LIST-S2	Unsupervised	0.842
26	MutationTaster	Supervised	0.816
27	DANN	Supervised	0.812
28	LRT	Unsupervised	0.805
29	FATHMM	Supervised	0.723

Table A17: **ProteinGym - Clinical substitution benchmark** Ranking based on AUROC between model prediction and ClinVar benign/pathogenic annotation.

Model Type	Model Name	AUROC(↑)	AUPRC (↑)
Alignment-based models	HMM	0.679	0.775
	PROVEAN	0.926	0.947
	WaveNet	–	–
Protein language models	UniRep	0.395	0.600
	RITA XL	0.923	0.954
	ProGen2 XL	0.846	0.889
	Tranception L (no retrieval)	0.877	0.938
	Tranception M (no retrieval)	0.858	0.929
	ProtGPT2	0.655	0.779
Hybrid models	Tranception L	0.857	0.920
	Tranception M	0.844	0.909
	TranceptEVE	0.857	0.916

Table A18: **ClinVar AUROC and Average Precisions** Results for indel-compatible baselines on our ClinVar/gnomAD indel benchmark. AUPRC is area under the precision recall curve, and AUROC is area under the receiver-operating characteristic curve.

Table A19: **List of substitution datasets** See the reference file in the GitHub repo for other info (UniProt ID, taxon, DOI, and more assay details).

Dataset	Reference
β -Lactamase	Jacquier et al. [2013]
β -Lactamase	Stiffler et al. [2015]
β -Lactamase	Firnberg et al. [2014]
β -Lactamase	Deng et al. [2012]
β -Lactamase VIM-2	Chen et al. [2020]
β -Glucosidase	Romero et al. [2015]
AAV	Sinai et al. [2021]
ACE2	Chan et al. [2020]
ADRB2	Jones et al. [2020]
APH(3')II, neo	Melnikov et al. [2014]
APP	Seuma et al. [2021]
Activation-induced deaminase	Gajula et al. [2014]
Aliphatic amidase	Wrenbeck et al. [2017]
Alpha-synuclein	Newberry et al. [2020]
Amyloid β	Gray et al. [2019]
Amyloid β	Seuma et al. [2022]
Ancestral spleen tyrosine kinase	Hobbs et al. [2022]
Anti-CRISPR protein AcrIIA4	Stadelmann et al. [2021]
Antitoxin ParD3	Ding et al. [2023]
Antitoxin ParD3	Aakre et al. [2015]
Arrestin-1	Ostermaier et al. [2014]
BRCA1	Findlay et al. [2018]
BRCA2	Erwood et al. [2022]
CALM1	Weile et al. [2017]
CARD11	Meitlis et al. [2020]
CASP3	Roychowdhury and Romero [2022]
CASP7	Roychowdhury and Romero [2022]
CBS (cystathionine beta-synthase)	Sun et al. [2020]
CCR5	Gill et al. [2023]
CD19	Klesmith et al. [2019]
CVB3 capsid	Mattenberger et al. [2021]
CXCR4	Gill et al. [2023]
Chalcone synthase	Wrenbeck et al. [2019]
Cytochrome P450 2C9	Amorosi et al. [2021]
Cytochrome P450 2C9	Amorosi et al. [2021]
D-amino acid oxidase	Vanella et al. [2023]
DHFR reductase	Nguyen et al. [2023a]
DHFR reductase	Thompson et al. [2020]
DNA methylase HaeIII	Rockah-Shmuel et al. [2015]
Dengue virus NS5	Suphatrakul et al. [2023]
Dlg4, (PSD95_PDZ3)	McLaughlin et al. [2012]
EfrC	Meier et al. [2023]
EfrD	Meier et al. [2023]
EnvZ	Ghose et al. [2023]
ErbB2 membrane domain	Elazar et al. [2016]
EstA	Nutschel et al. [2020]
GAL4	Kitzman et al. [2015]
GB1	Wu et al. [2016]
GB1	Olson et al. [2014]
GDI1	Silverstein et al. [2021]
GFP	Sarkisyan et al. [2016]
GMR (aacC1)	Dandage et al. [2018]
GRB2-SH3	Faure et al. [2022]
Gcn4	Staller et al. [2018]
Glucokinase regulatory protein	Gersing et al. [2023]
Glucokinase regulatory protein	Gersing et al. [2022]
Glycophorin A membrane domain	Elazar et al. [2016]
Green fluorescent protein amacGFP	Gonzalez Somermeyer et al. [2022]
Green fluorescent protein cgreGFP	Gonzalez Somermeyer et al. [2022]
Green fluorescent protein plluGFP2	Gonzalez Somermeyer et al. [2022]

Table A19: (continued)

Dataset	Reference
HIV env	Duenas-Decamp et al. [2016]
HIV env	Haddox et al. [2018]
HIV env (BF520)	Haddox et al. [2018]
HIV env (BG505)	Haddox et al. [2018]
HIV rev	Fernandes et al. [2016]
HIV tat	Fernandes et al. [2016]
HMG-CoA reductase	Jiang [2019]
HRAS	Bandaru et al. [2017]
HSP82	Flynn et al. [2020]
HSP82	Mishra et al. [2016]
Hsp90	Hietpas et al. [2011]
Hydroxymethylbilane synthase	van Loggerenberg et al. [2023]
IGP dehydratase (HIS3)	Pokusaeva et al. [2019]
InfA	Kelsic et al. [2016]
Influenza H3N2 neuraminidase	Lei et al. [2023]
Influenza M1 matrix protein	Hom et al. [2019]
Influenza RNA polymerase PB1	Li et al. [2023]
Influenza hemagglutinin	Thyagarajan and Bloom [2014]
Influenza hemagglutinin	Doud and Bloom [2016]
Influenza hemagglutinin	Wu et al. [2014]
Influenza hemagglutinin	Lee et al. [2018]
Influenza neuraminidase	Jiang et al. [2016]
Influenza nucleoprotein	Bloom [2014]
Influenza nucleoprotein	Doud et al. [2015]
Influenza nucleoprotein	Doud and Bloom [2016]
Influenza polymerase acidic protein	Wu et al. [2015]
Influenza polymerase basic protein 2	Soh et al. [2019]
KCNE1	Muhammad et al. [2023]
KCNH2	Kozek et al. [2020]
KCNJ2	Coyote-Maestas et al. [2022]
KRAS	Weng et al. [2022]
KRAS	Ursu et al. [2022]
L-selectin	Elazar et al. [2016]
LGK (levoglucosan kinase)	Wrenbeck et al. [2019]
LGK (levoglucosan kinase)	Klesmith et al. [2015]
LamB	Andrews and Fields [2020]
Leucine-rich repeat protein SHOC-2	Kwon et al. [2022]
MAPK1	Brenan et al. [2016]
MET kinase	Estevam et al. [2023]
MPL	Bridgford et al. [2020]
MSH2	Jia et al. [2021]
MTHFR reductase	Weile et al. [2021]
MlaC	MacRae et al. [2023]
NPC intracellular cholesterol transporter	Erwood et al. [2022]
NPC intracellular cholesterol transporter	Erwood et al. [2022]
NS5A	Qi et al. [2014]
NUDT15	Suiter et al. [2020]
OCT1 (SLC22A1)	Yee et al. [2023]
Ornithine transcarbamylase	Lo et al. [2023]
p53	Giacomelli et al. [2018]
p53	Kotler et al. [2018]
PAB1	Melamed et al. [2013]
PPARG	UK Monogenic Diabetes Consortium et al. [2016]
PSD95-PDZ3	Faure et al. [2022]
PTEN	Matreyek et al. [2021]
PTEN	Mighell et al. [2018]
Parkin	Clausen et al. [2023]
Phosphoserine aminotransferase	Xie et al. [2023]
Phototropin	Chen et al. [2023]
Pilin (Pile)	Kennouche et al. [2019]
Plasminogen activator inhibitor-1	Huttinger et al. [2021]

Table A19: (continued)

Dataset	Reference
Protein phosphatase 1D	Miller et al. [2022]
RAF oncogene	Zinkus-Boltz et al. [2019]
RNase III (rnc)	Weeks and Ostermeier [2023]
Rhodopsin	Wan et al. [2019]
SARS-CoV-2 Mpro	Flynn et al. [2022]
SARS-CoV-2 Spike RBD	Tan et al. [2023]
SARS-CoV2 Spike RBD	Starr et al. [2020]
SCN5A	Glazer et al. [2020]
SOX17	Veerapandian et al. [2018]
SOX2	Veerapandian et al. [2018]
SRC	Ahler et al. [2019]
SUMO-conjugating enzyme UBC9	Weile et al. [2017]
Small ubiquitin-related modifier 1	Weile et al. [2017]
Sodium-dependent serotonin transporter	Young et al. [2021]
Src	Chakraborty et al. [2021]
Src	Nguyen et al. [2023b]
Streptococcus pyogenes Cas9	Spencer and Zhang [2017]
TARDBP	Bolognesi et al. [2019]
TIM Barrel (S. solfataricus)	Chan et al. [2017]
TIM Barrel (T. maritima)	Chan et al. [2017]
TIM Barrel (T. thermophilus)	Chan et al. [2017]
Thiamin pyrophosphokinase 1	Weile et al. [2017]
Thiopurine S-methyltransferase (TPMT)	Matreyek et al. [2018]
Toxin CcdB	Tripathi et al. [2016]
Toxin CcdB	Adkar et al. [2012]
Tsuboyama multi-DMS	Tsuboyama et al. [2023]
Ube4b	Starita et al. [2013]
Ubiquitin	Roscoe et al. [2013]
Ubiquitin	Roscoe and Bolon [2014]
Ubiquitin	Mavor et al. [2016]
VKORC1	Chiasson et al. [2020]
VKORC1	Chiasson et al. [2020]
YAP1	Araya et al. [2012]
Zika virus env	Sourisseau et al. [2019]

Dataset	Reference
β -Lactamase	Gonzalez et al. [2019]
AAV	Sinai et al. [2021]
Chorismate mutase (CM)	Russ et al. [2020]
IGP dehydratase (HIS3)	Pokusaeva et al. [2019]
Kir2.1	Macdonald et al. [2023]
MtrA	Campbell et al. [2022]
p53	Kotler et al. [2018]
PTEN phosphatase	Mighell et al. [2018]
amyloid β	Seuma et al. [2022]
OCT1 (SLC22A1)	Yee et al. [2023]
Tsuboyama multi-DMS	Tsuboyama et al. [2023]

Table A20: **List of indel datasets.**